DISLOCATION DYNAMICS SIMULATIONS OF PLASTICITY IN Cu THIN FILMS

Han Wu

Thesis Prepared for the Degree of

MASTER OF SCIENCE

UNIVERSITY OF NORTH TEXAS

August 2013

APPROVED:

Zhiqiang Wang, Major Professor
Marcus Young, Committee Member
Zhenhai Xia, Committee Member
Jincheng Du, Departmental Graduate Advisor
Nigel Shepherd, Interim Chair of the Department of Materials Science and Engineering
Costas Tsatsoulis, Dean of the College of Engineering
Mark Wardell, Dean of the Toulouse Graduate School

Wu, Han. *Dislocation Dynamics Simulations of Plasticity in Cu Thin Films*. Master of Science (Materials Science and Engineering), August 2013, 47 pp., 2 tables, 44 figures, 54 numbered references.

Strong size effects in plastic deformation of thin films have been experimentally observed, indicating non-traditional deformation mechanisms. These observations require improved understanding of the behavior of dislocation in small size materials, as they are the primary plastic deformation carrier. Dislocation dynamics (DD) is a computational method that is capable of directly simulating the motion and interaction of dislocations in crystalline materials. This provides a convenient approach to study micro plasticity in thin films. While two-dimensional dislocation dynamics simulation in thin film proved that the size effect fits Hall-Petch equation very well, there are issues related to three-dimensional size effects. In this work, three-dimensional dislocation dynamics simulations are used to study model cooper thin film deformation. Grain boundary is modeled as impenetrable obstacle to dislocation motion in this work. Both tension and cyclic loadings are applied and a wide range of size and geometry of thin films are studied. The results not only compare well with experimentally observed size effects on thin film strength, but also provide many details on dislocation processes in thin films, which could greatly help formulate new mechanisms of dislocation-based plasticity.

ACKNOWLEDGEMENTS

First of all, I would like to thank Prof. Zhiqiang Wang for his patience and sincere care in these several years. You always pardoned my laziness and encouraged me to have large progress. I would also like to express my gratitude to Prof.Xia and Prof.Young to be my committee member. My special thanks also go to every group member for the fruitful discussions which enlightened me in my research. Last but not least, I also like to thank all the members of our great organization----—Lunch Party‖. We have enjoyed a wonderful time which I will never forget. Our friendship will last forever. Love you all.

TABLE OF CONTENTS

Page

LIST OF TABLES

Page

LIST OF ILLUSTRATIONS

Page

CHAPTER 1

INTRODUCTION

A tremendous amount of experimental research has been carried out with respect to mechanical properties of materials. However, with the recent technological developments, computational modeling techniques now can provide significant advantages to material deformation research.

The primary advantages of computational methods, which they are (1) less-time consuming (2) eliminate the need for expensive experimental instruments (3) various design models. Hence, computational methods are widely applied to the field of materials science and engineering. In this work, the parametric dislocation dynamics code which was developed by Ghoniem and coworkers to solve dislocation dynamics problem on single crystal copper, is used [2, 4-11, 19, 42, 50]. In this chapter, the micro scale mechanical theory, the size effect, the application of thin film in industrial and scientific fields, and dislocation dynamics theory are discussed. In addition, the details of the methods including dislocation dynamics simulation code are introduced. In the subsequent chapters, several models and some results are discussed, i.e. comparisons between fixed boundary and free surface cases and tension and compression cases. The conclusions and future research are given in the last two chapters.

1.1 Micro Scale Application

The concept of multi-scale material plasticity has been introduced in recent years to increase the understanding of material strength dependence with time and size. The concept includes meso scale, micro scale, continuum scale and atomistic scale calculations.

For example, the semiconductor industry has played a major role in micro scale applications which are used in various electrical instruments such as radio, LED TV, solar panel, solar cell, etc.

1.2 Thin Film Technology

Thin films are often used in modern scientific applications. Single crystal, poly crystal, organic and inorganic material can all be designed as thin films with thickness ranging from 10^{-3}μm to 10^{-6}μm for ultra-thin films.

Thin film technology and its application show prosperous development. For example, diamond thin film, which has excellent mechanical properties like hardness, stiffness, conductivity, and the modulus of elasticity, can be used in cutting instruments, hard drive protectors, and insulators for electronic devices. Intelligent material thin films usually contain several kinds of materials such as metals and metallic alloys, ceramics, and polymers. Starting in the 1990s, bio-technology has been introduced into intelligent material thin films. Moreover, nano-phase material thin films have excellent optical and gas-sensitive properties.

1.3 Size Effect

As discussed above, the mechanical properties of metallic thin films are typically of higher standards then the bulk material and hence have excellent applications in both microelectronic and micro-electro-mechanical devices. Contrary to bulk materials, it has been found that the strength of metallic thin films can be influenced by dislocation microstructures. Furthermore, the yield strength depends strongly on grain size. Hall (1951) and Petch (1953) first realized that the yield strength is governed by the square root of average grain size, i.e. $d^{-1/2}$. Subsequently, plenty of practical experiments have confirmed this relationship. These experiments included fracture toughness tests, flow stress tests, fatigue tests etc. The relationship between flow or yield stress and grain size can be written as

$$\sigma = M\tau = M(\tau_0 + Kd^{-1/2}) \quad (1)$$

where σ is the yield stress, M is the Taylor orientation factor and τ_{crss} is the critically resolved shear stress[53].

In this study, the behavior of dislocations in single crystal copper will be studied. Two models are used to explain the size effect in thin films. The first model is Nix-Freund model, which assumes that only a part of dislocation is forced to deposit

on the interface. The second model is Hall-Petch model in which dislocations are allowed to pile-up at the interface [2]. The Hall-Petch model has been chosen in the current research work. Dislocation pile-ups upon the force field lead to accumulation of high energy at the grain boundary, and as a result drive the material to undergo plastic deformation. In the recent past, 2D discrete dislocation simulations in thin film have been abundantly used to study this effect [1]. However, the present study uses three-dimensional dislocation dynamics simulations to study deformation in cooper thin films.

CHAPTER 2

RELATIVE LITERATURE REVIEW

2.1 Previous Experimental Progress in Relative Study

In previous thin film plastic deformation experiments, thin films were classified to be passive or un-passive. Plane-strain bulge test was used to obtain stress-strain relationship through pressure deflection behavior on thin films [3]. In order to reduce the amount of thin film required, silicon micromachining technology has been often used. The surface of the thin film can be treated with electroplated or sputtered in order to prevent it from oxidization. TaN/Si_3N_4 is usually used as coating before sputtering, and the Ar plasma for cleaning. TaN/Si_3N_4 is strongly proved to be stable after the sample was treated in dilute nitric acid. These films were then subjected to mechanical testing, including both tension and cyclic tests. Transmission electron microscopy (TEM) is a significant tool to obtain further grip on the microstructural detail inside the material.

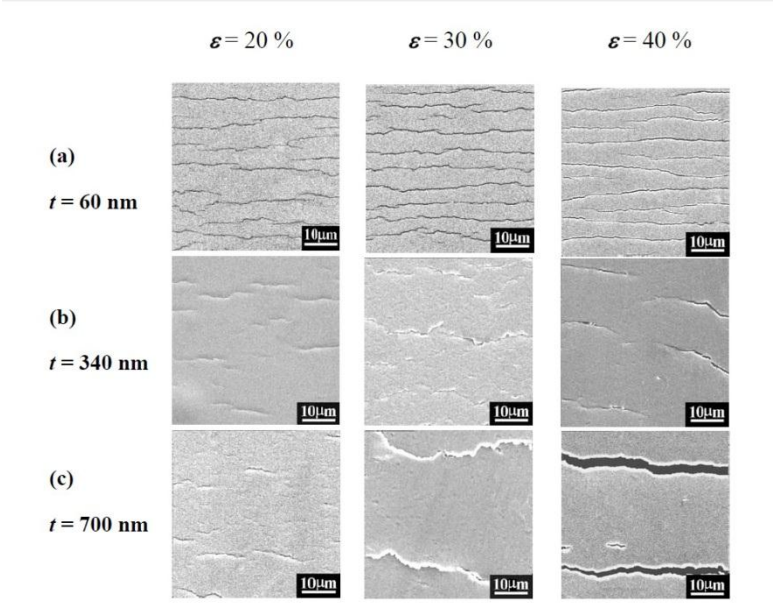

Fig.1 Microstructural evolution of 60 nm, 340 nm , and 700 nm thick Cu films [14]

In Niu's work [14], the dependence of critical strain on the film thickness for polycrystalline Cu under tensile loading condition was studied. Fig 1 is a TEM

microstructure graph, shows that at same strains, crack density would decrease as the thickness increases. In other words, for thinner film, dislocations are more likely to pile-up at the boundary. Fig 2 shows the plane-strain bulge test.

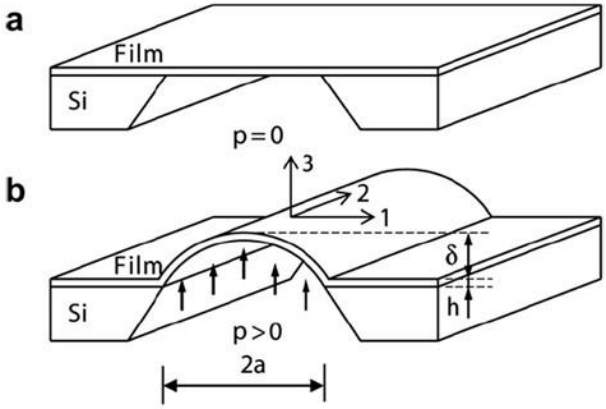

Fig.2 Simple illustration of plane strain-bulge test [15].

In Xiang's work [15], after experiment, films with a passivation layer on one or both surfaces have yield stress that increases significantly with decreasing film thickness [15], as shown in Fig 3 below.

Table 1
Summary of the experimental results

Film set	Thickness h (μm)	Average grain size[a] d (μm)	h/d	Passivation[b]	Yield stress[c] σ_y (MPa
First set, electroplated	4.20 ± 0.05	1.50 ± 0.05	2.80 ± 0.13	Yes	181.8 ± 3.5
				No	175.5 ± 3.7
	1.90 ± 0.05	1.51 ± 0.04	1.26 ± 0.07	Yes	212.6 ± 4.5
				No	200.2 ± 4.1
	1.00 ± 0.05	1.50 ± 0.05	0.67 ± 0.04	Yes	250.8 ± 5.4
				No	200.5 ± 4.2
Second set, sputtered	0.89 ± 0.01	0.46 ± 0.02	1.93 ± 0.11	Yes	335.5 ± 16.8
				No	250.3 ± 12.5
	0.67 ± 0.01	0.46 ± 0.01	1.43 ± 0.05	Yes	373.6 ± 16.7
				No	266.1 ± 13.3
	0.61 ± 0.01	0.54 ± 0.02	1.14 ± 0.06	Yes	434.6 ± 21.7
				No	299.7 ± 15.0
	0.44 ± 0.01	0.39 ± 0.01	1.13 ± 0.05	Yes	611.7 ± 30.6
				No	346.6 ± 17.3
	0.34 ± 0.01	0.33 ± 0.01	1.06 ± 0.06	Yes	695.5 ± 34.8
				No	365.6 ± 18.3

[a] The average grain size was determined by the intercept method with twins counted as separate grains.
[b] The passivation consists of 20 nm Ti on both surfaces for electroplated films and 80 nm Si_3N_4/20 nm TaN on one surface for sputtered films.
[c] The yield stress is defined at 0.2% offset strain for all films.

Fig.3 Plane strain-bulge test result in experiment for electroplated and sputtered treated surfaces[15].

The electroplated and sputtered treatments methods are used to treat thin film surfaces. Fig 3 shows that for passivation surface, thinner thickness film always has

higher yield stress. Also the films with passivation have a significantly larger flow stress than un-passivated films [15].These phenomena are shown in Fig 4.

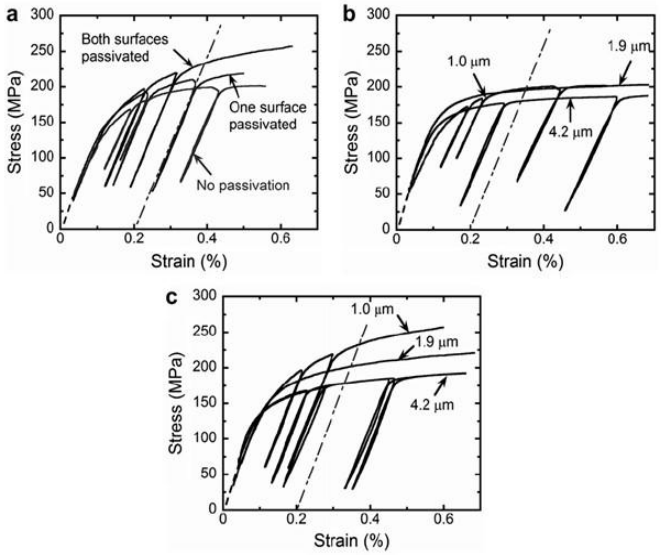

Fig.4 (a)The effect of passivation on the stress–strain curves of 1.0 lm electroplated Cu films. (b)The effect of film thickness on the stress–strain curves of electroplated Cu films without surface passivation. (c)The effect of film thickness on the stress–strain curves of electroplated Cu films with both surfaces passivated by 20 nm of Ti[15].

The Bauschinger effect for passive thin film is stronger and stronger for passive thinner films as well [15].

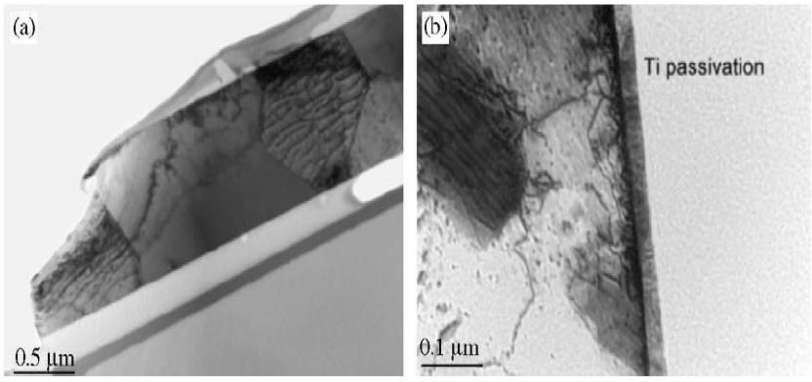

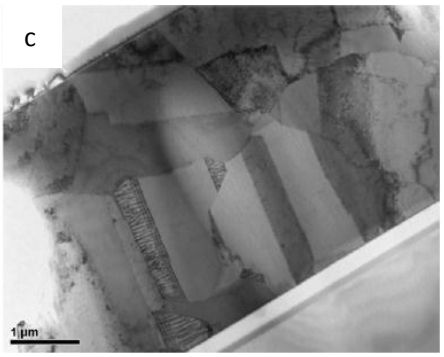

Fig.5 TEM picture for Cu of (a).1.0μm (b) 1.9μm (c) 4.2μm[15]

And Fig 5 shows larger thickness thin film has larger grain size.

2.2 Previous Research about 2D Model of Thin Films and Size Effect

Dislocations, originally established in 1930s are one dimensional defect which are usually formed in atom-scale. Computational Modeling is a powerful method which utilizes super computers to simulate virtual model of the material system and is widely used in physics, astrophysics, chemistry and biology [19].

Charles Frank and Thornton Read proposed Frank Read source model which explains the dislocation motion in specific slip plane under deformation. When external force field is applied on Frank-Read source, dislocations are primarily generated and move along their slip planes. Cold work of metals can increase the number of dislocations through this mechanism. Higher dislocation density can largely increase the yield strength and cause working hardening. Fig 6 shows the Frank-Read model and how the dislocation loop is formed upon loading will move under external loading.

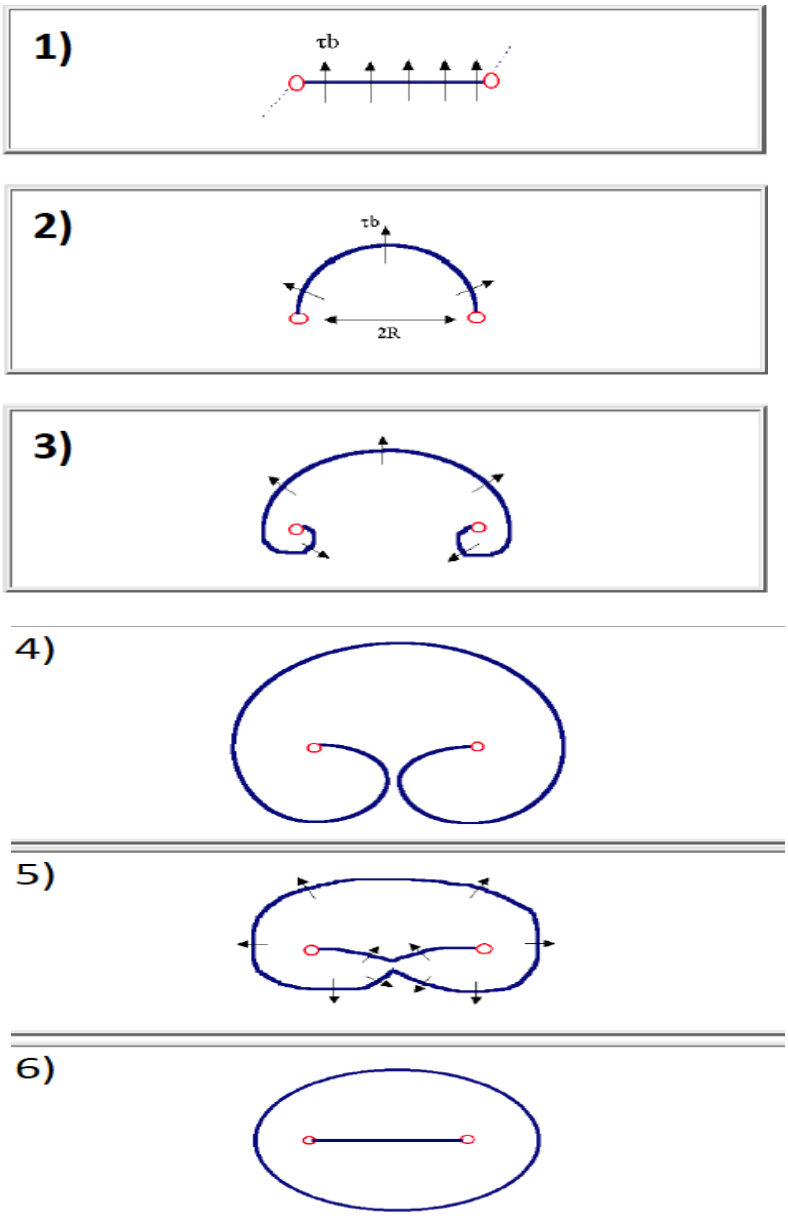

Fig.6 Different stages of Frank Read source under deformation. (1) Initial. (2)(3) Dislocation responds to the force by bowing out. (4) Same burgers vector, different line direction. (5) Annihilation. (6) Close loop and form a new source.

A Frank Read source is activated by a force $F = \tau b$, where b is the burgers vector and τ is resolved shear stress. The dislocation begins to move parallel or perpendicular to the direction of burgers vector [39, 40].Fig 6 shows the motion picture for Frank-Read source. As the movement continues, parts of dislocation lines are very close to each other. When the distance between these parts are smaller than a certain distance (smaller than $n \bullet b$, n usually varies from 0 to 10 [2], it will result in

dislocation annihilation, which in turn leads to a formation of a new loop and new source and so on. This dislocation slip model is one of the most crucial concepts on which dislocation dynamics is based on.

Thin film dislocation dynamics has been originated from 2D model. Thermal mismatch is the main reason for plastic deformation. Different from 3D crystal structure slip system, 3 slip planes which has 60° angle between each other has been set up before as shown in Fig.7[3].

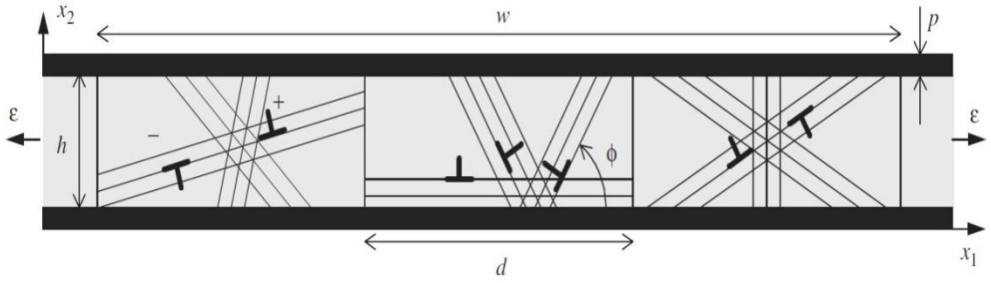

Fig.7 Two-dimensional model of a freestanding film passivated on both sides under tensile loading[3].

Strain-gradient theory was established by Hutchinson and co-workers in 1933, which had significant influence to the size effect. It is motivated by the fact that a well-adhered passivation layer can prevent dislocations from going out of the film and lead to a plastic strain gradient near the film–passivation interface. For micron scale, plastic strain gradients can increase the resistance to plastic flow by increasing the dislocation density [16].Plastic deformation in crystal solid is caused by large number of dislocation motion and accumulation [17].

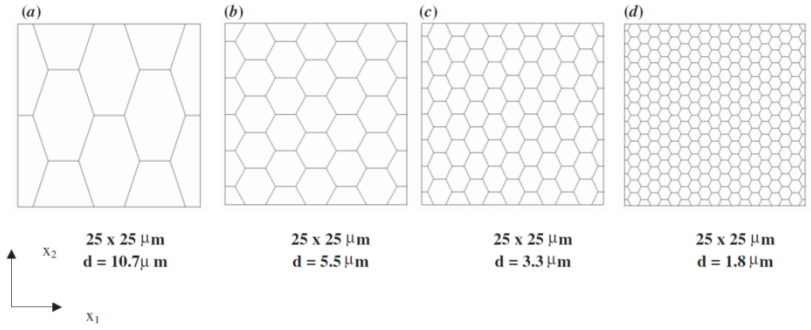

Fig.8 Simulation 2D case model for Cu. [17]

For 2D model,as shown in fig 8, the first challenge is how to define the slip system. And connection areas between grain boundaries and slip planes are treated as the obstacle of dislocation motion. When the distance between the obstacle and dislocation line is smaller than 10 times of burgers vector of the dislocation, the dislocation will then be made to stop. If distance between the two dislocations becomes smaller than 6 times of burgers vector of the dislocation, it leads to dislocation annihilation [17].Fig 9 shows the dislocation simulation image after shear loading [17].

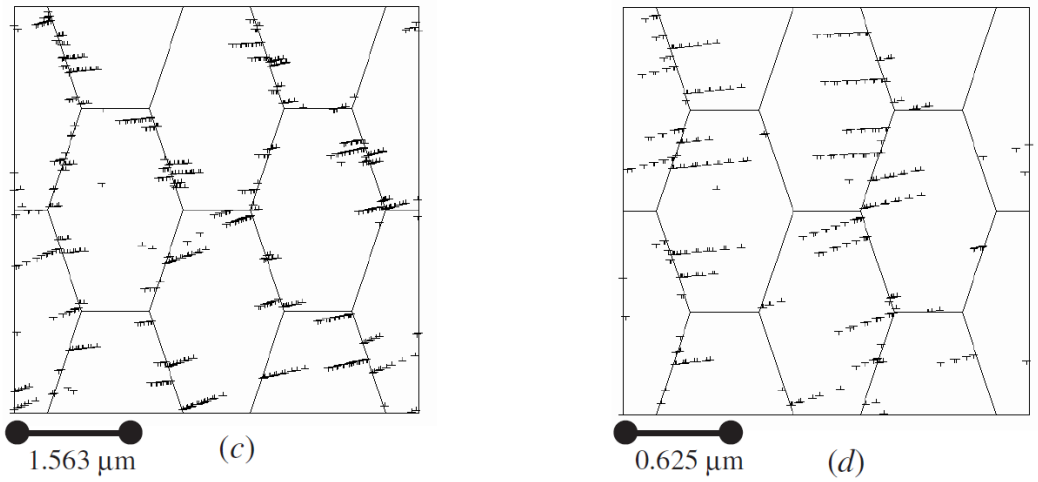

Fig.9 Simulation dislocation image for two kinds of thickness thin film[17].

It shows that when the grain size decreases, the number of sources being activated will be larger. Dislocation densities will increase almost linearly as the loading continues. Fig 10 shows the shear strain vs. stress in S. B. Biner's work.

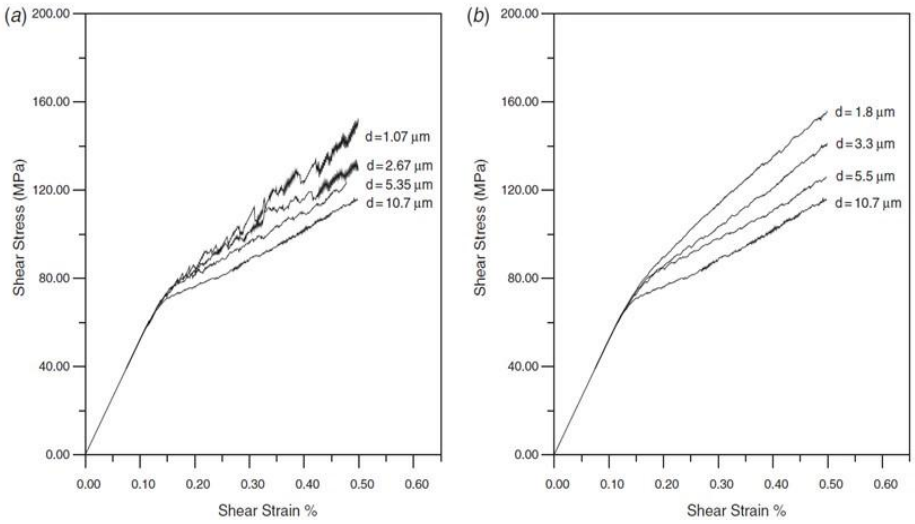

Fig.10 Shear strain-stress plot for different grain size. (a)constant morphology and different unit-cell size. (b) constant size and different morphology [17]

In fig 10, no matter if it is same grain size/different morphology or same morphology/different grain size, the size-effect is always observed. In addition, the large curve fluctuation in the simulation states that, strain-control is the dominant simulation condition rather than displacement control.

The dislocation source density and initial configuration position do not affect the Hall-Petch relationship [17], which in turn suggests that the simulation dislocation source position which is randomly distributed or particularly distributed may not influence the mechanical properties of thin film.

2.3 3D Simulation Background about Size Effect

Contrary to 2D thin film study, 3D model dislocation dynamics study has made good progress less than a decade ago. In 3D dislocation dynamics simulations, there are two kinds of dislocation model; one is Nix–Freund model which assumes that when dislocation passes through the film surface/interface/grain boundary, it will be forcibly deposit on those places. The other is Hall-Petch behavior model which assumes dislocations would pile-up at the grain boundary or interface [18, 20, 21, 22, 23, 24]. Previous discussions show that for freestanding thin film, yield strength will not be largely influenced by thin film thickness [27]. Thus in 3D model, we assume that the dislocation motion is stopped at the boundary according to the Hall–

Petch-behavior. Fig 11 is how the dislocation motion be affected under the Hall–Petch-behavior model at the boundary.

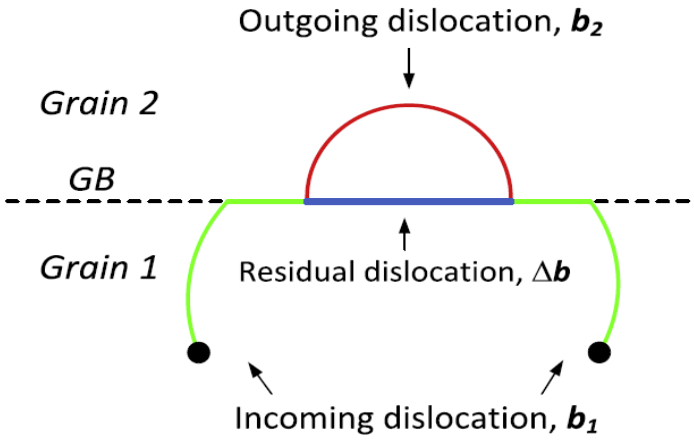

Fig.11 How the dislocation moves when it hit grain boundary[2].

Dislocations may be blocked, reflected, absorbed or transmitted at grain boundaries. When the incoming dislocation b_1 hit the grain-boundary; part of dislocation will be absorbed. The rest will elect a new dislocation based on the previous one and interact with boundary. The microstructure picture of dislocation motion at fix boundary can be partly concluded rom the multi-grain case. In mechanical aspect, this is how the boundary condition is clearly classified, which uses two parameters---the GB transmission strength τ_{GB} and the critical stress to activate the FR sourceτ_{FR}. If the ratio of τ_{GB} and τ_{FR} is equal to positive infinite number, that represents a fix boundary condition [2].

For a close boundary case in face center cubic multi-grain copper, under tensile loading condition, the strain-stress curve is shown in fig 12[2].

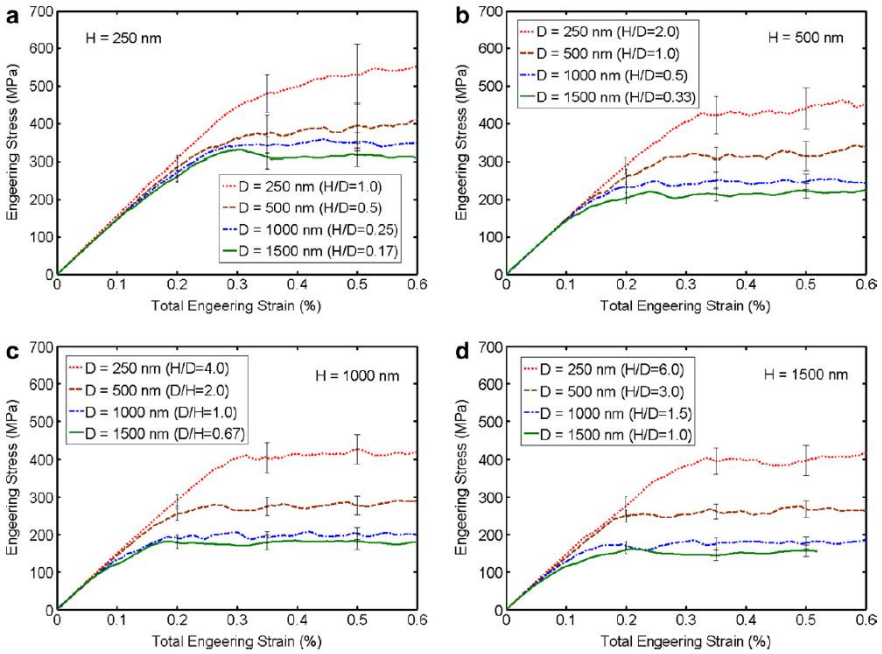

Fig.12 Engineering strain-stress curve for different height simulation sample[2].

From Fig 13, smaller height (H) case has larger yield strength. And for the same H, smaller size always has larger yield strength. The microstructure picture, fig 13, shows that as deformation continues, more dislocations would pile-up at the boundary. In addition to that, for films with a higher aspect ratio (H/D), more dislocations would be stored at the boundary area [2].

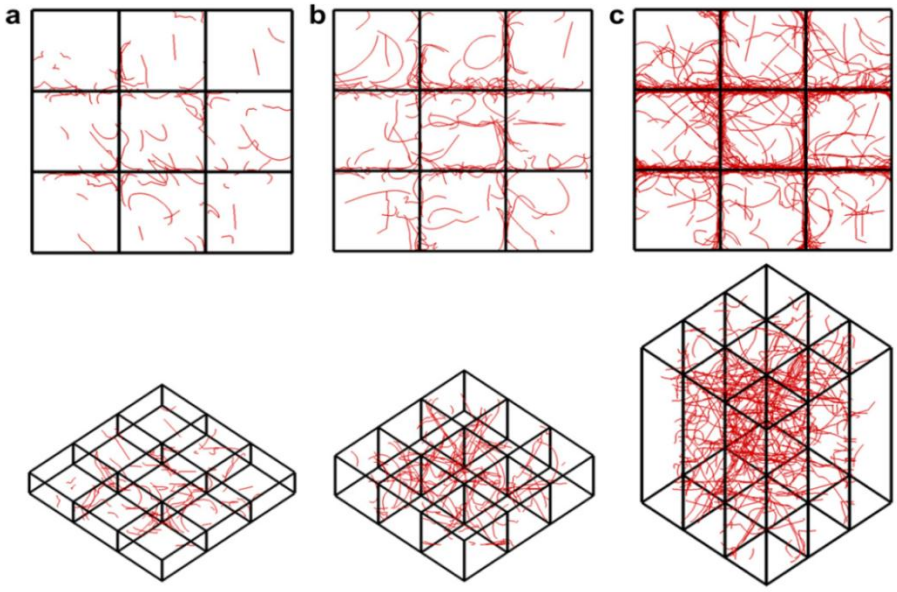

Fig.13 Dislocation structures in films with a grain size equal 500 nm under 0.5% strain and different film thicknesses. The upper figures upper are in a [001] view, while the lower are in

a [111] view: (a) thicknesses equal 250nm (H/D = 0.5); (b) thicknesses equal 500nm (H/D = 1.0; (c) thicknesses equal 2000nm (H/D = 4.0) [2]

CHAPTER 3

MODEL SETUP AND SIMULATION CONDITION

3.1 Parametric Dislocation Dynamic Method

Originally designed by Ghoniem and coworkers, this method uses a serial computing program in order to perform multiple calculations simultaneously [2, 4, 5, 6, 8, 11, 42]. Applying this method, large calculations can be divided into some smaller parts to increase the calculation speed; however, improvements are yet to be made in terms of the communication between different processors.

Due to rapid development in computer technology, building a computer cluster is a lot more robust. Communication can be successfully achieved from cluster nodes by message passing interface (MPI) computer language [45, 46, 47, 48].

A numerical equation has been derived to calculate the force on the dislocation, which is consisted of Peach-Koehler force, self-force, and Osmotic force. Based on these calculations, the resulting microstructure graph is directly observed in the simulations [5].

In dislocation dynamics, discrete dislocations are set as straight lines [12, 13, 19, 20, 21, 22, 23, 24, 42] and using the Peach-Koehler force, as shown in the Fig 14.

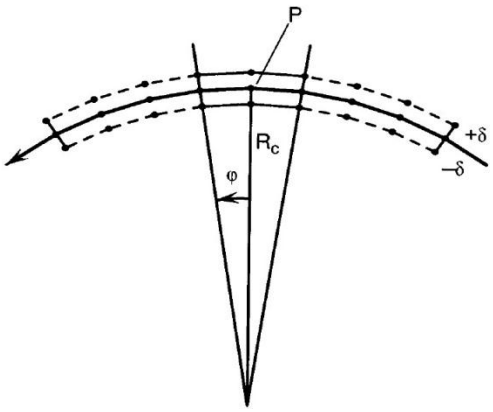

Fig.14 Finite-core treatment used in this article. The point of interest P and its nearest neighbors define a circle with a radius of curvature Rc . The contributions from the two displaced arcs are shown as solid lines [13].

In addition, if the self-force is considered in the model, the curvature of dislocation is required in the model since self-force function is based on the curvature of dislocation line [5, 49, 50].

The biggest advantage of parallel computing is to let the computer run different parts of calculation at the same time. Fig 15 shows the tree structure of parallel computing.

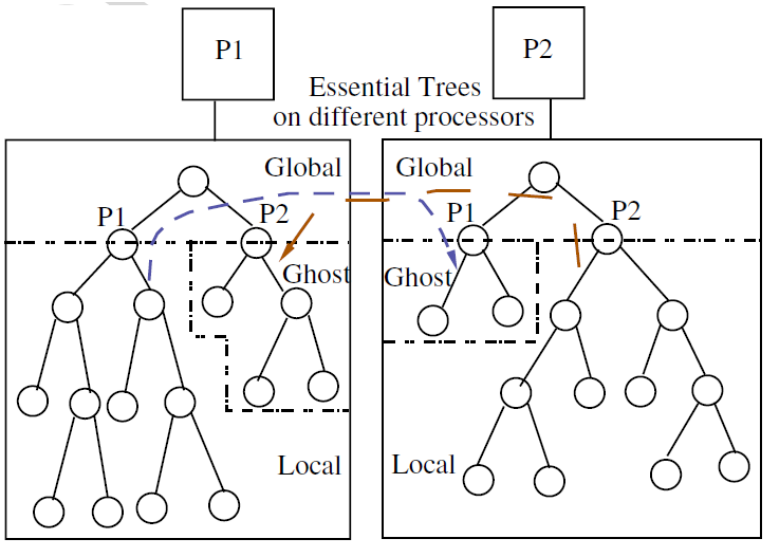

Fig.15 Tree structure on processor. Global processor assigns jobs to slave processor, and communicate the computing information[11].

The equation of motion of dislocation is derived from Gibbs free energy theory as

$$\int_{\Gamma} (F_k^t - B_{\alpha\kappa} V_\alpha) \delta r_k |ds| = 0 \qquad (2)$$

The forces F set in the code consist of three parts. $B_{\alpha\kappa}$is resistive matrix; V_α is velocity of the dislocation motion; r_k is position of a point on dislocation[31, 32, 33]. The force of this model---F_k^t, which is the Peach-Koehler force, can be written as

$$f_{PK} = b \cdot \sum \times t \qquad (3)$$

where b,$\sum$ and t are burgers vector of dislocation, applied stress field from interaction of dislocations and external stress, and tangent vector of dislocation line, respectively [11].

In order to predict the accurate position and reflect the motion trend of dislocations,

dislocation lines are uniformly divided into many segments. The position and tangent vector together describe the movement of two mathematical nodes. Furthermore, the whole dislocation motion can be summarized by sufficient number of nodes, as in Fig 16.

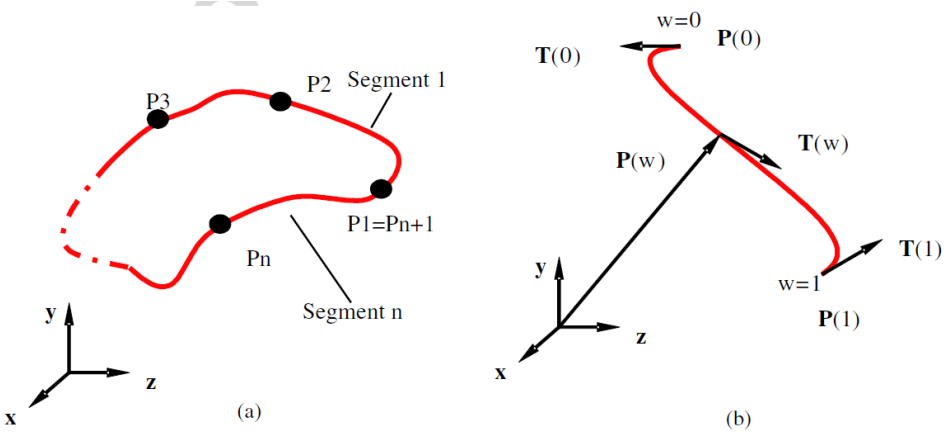

Fig.16 Dislocation line simulation graph. (a) nodes on dislocation line. (b) two nodes as the corer points [11]

Equation (2) can be written as a function of global resistivity matrix and dislocation line [5]. It is

$$\mathcal{F}_k = \sum_{l=1}^{N_{tot}} \Gamma_{kl} l_{l,t} \tag{4}$$

After solving the equation (4), the coordinates and dislocation shape can be generated by number integration method [4, 5]. Also, from the equation (3) and the model we want to set, a fast sum method is used to show the accurate dislocation geometry, which is developed by Ghoniem and co-workers [4]. Fig 17 shows how the stress field is computed on the dislocation line.

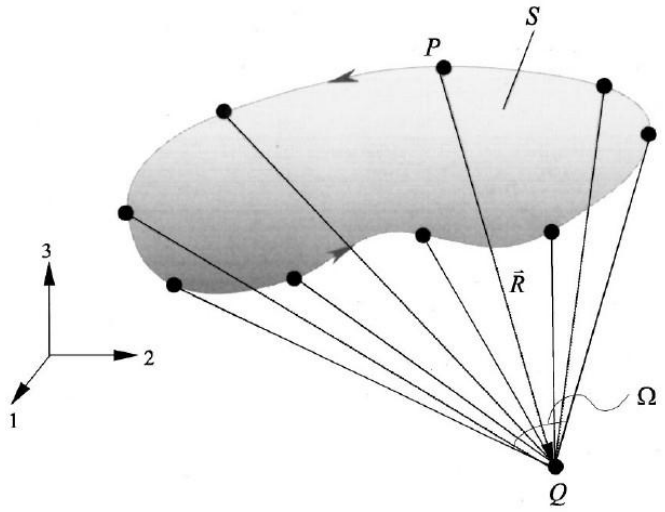

Fig.17 Solid angle (Ω) at a field point (Q),and how is the relationship with the dislocation line containing point(P) [4]

The equation (3) can be re-written as

$$F_k = \sum_{l=1}^{N_{total}} \Gamma_{kl} Q_{l,t} \tag{5}$$

whereF_k is the force load, $\Gamma_{kl}$is the resistivity matrix and coordinates of dislocation nodes corresponds the symbol$Q_{l,t}$. The whole dislocation geometry in system can be determined by solving the equation. It can be used in both 2D and 3D model.
From the equation (4), the two global parameters---resistivity matrix and force matrix are assembled with the help of a local effective resistivity and an effective force. After solving the equation with finite element method (FEM), equation of motion can be summarized and re-written as the matrix function of global resistivity and coordinates for one dislocation node. [5] Then use Gauss–Jacobi or Gauss–Seidel iteration method[41, 43, 50, 52] to solve the force vector and resistivity at each time step for individual nodes which have the dislocation line connection, we arrive at equation (6)

$$S_i Q^p_{i,t+\delta t} = F_i - (S_{i-1} Q^{p-1}_{i-1,t} + S_{i+1} Q^{p-1}_{i+1,t}) \tag{6}$$

The above equation is applied on each dislocation particle i at time step$t + \delta t$, and p is iteration steps. Fig 18 is the relationship table for S and F of 3 segments on Frank Read source [5],

	S_{i-1}	S_i	S_{i+1}	F_i
l_1	0	γ_{11}^1	γ_{12}^1	f_1^1
l_2	γ_{21}^1	$\gamma_{22}^1+\gamma_{11}^2$	γ_{12}^2	$f_2^1+f_1^2$
l_3	γ_{21}^2	$\gamma_{22}^2+\gamma_{11}^3$	γ_{12}^3	$f_2^2+f_1^3$
l_4	γ_{21}^3	γ_{22}^3	0	f_3^2

Fig.18. Illustration for the calculation of resistivity and force elements for dislocation particles [5]

which are divided among 4 nodes [5]. That means each dislocation node has identified contribution about position, tangent vector, slip plane and burgers vector. Solve the information of those nodes; the data for the whole dislocation loop can be clear enough.

Also, in order to fulfill the function of passive surface, from equation 2 it is obvious that velocity is equal to zero, being the necessary condition for fix boundary. Since there are 2 coordinates in system, one is the slip plane which only have x and y on "plane", the other is the big coordinate system for whole material simulation sample, a transfer matrix is required.

3.2 Simulation Model and Boundary Condition Setup

This thesis will focus on single grain of metal crystalline. Two simulation groups are chosen in order to be convenient to compare---5μm thin film and 10μm film group. The thickness goes from 1μm to 5μm. So there are 10 groups of data total. Loading direction is positive x-axis [100]. For single crystal copper, shear modulus =50GPa, possion's ratio=0.34, lattice constant: 0.36nm. Slip system for FCC system is what we have already known---1/2<011> {111}. Dislocation density is $2\times10^7 cm/cm^3$. One more problem needs to mention here is dislocation sources are usually generated by computer code. Cubic is much easier to generate sources file. However, for thin film

which has “not so regular” slip system, the position of dislocation source has to be manually calculated by hand. In section 2.2 parametric Dislocation Dynamic Method has been discussed. So the only thing is to get the accurate position for dislocation nodes. The method for getting the thin film is cutting $5\times5\times5\mu m^3$ and $10\times10\times10\mu m^3$ cubic along [010] direction. Then set thin film to four $2.5\times2.5\times2.5\mu m^3$ and $5\times5\times5\mu m^3$ small octahedral shape. After that, in the center of octahedral shape, take $1\times1\times1\mu m^3$ small cubic out, as shown in Fig 19.

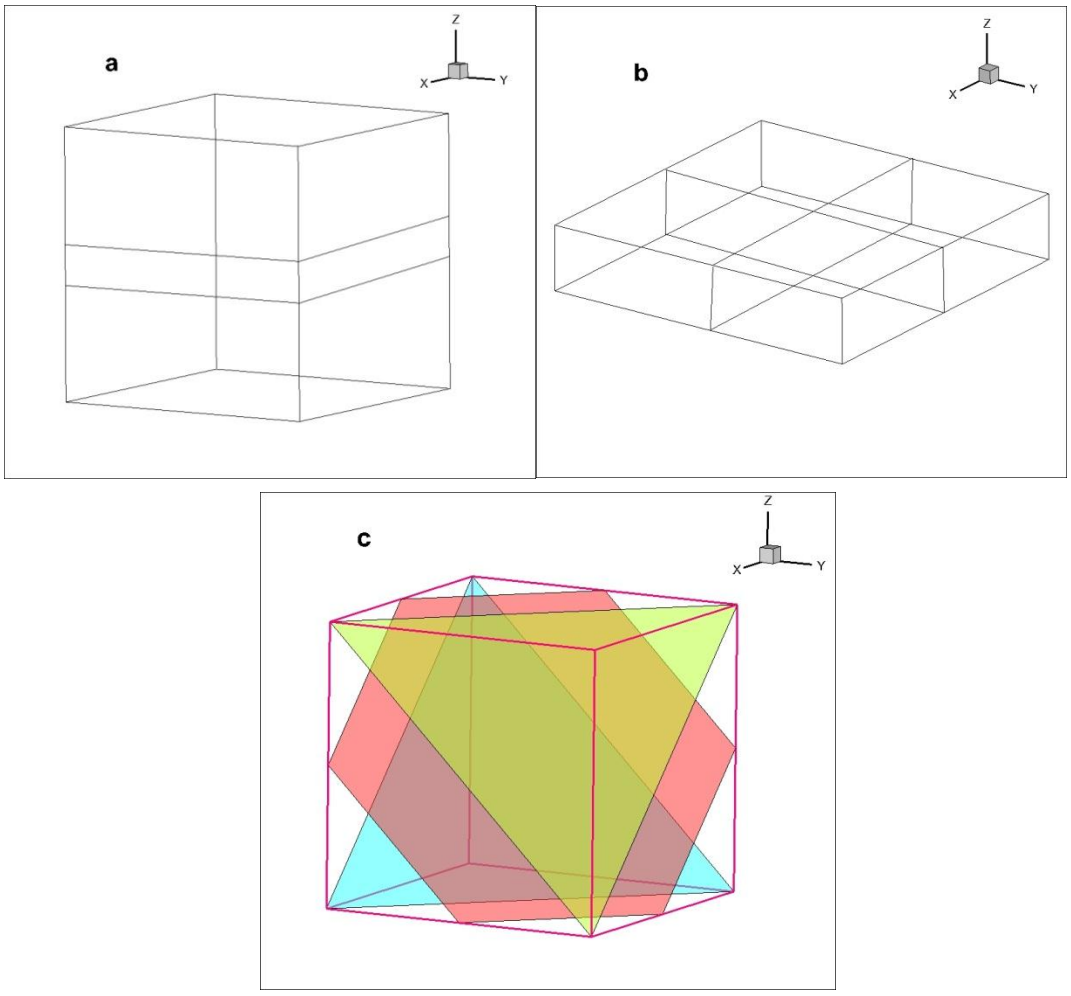

Fig.19 The method for taking thin film out from the big cubic. (a) Simulation cubic. (b) Simulation thin film. (c) Simulation small cubic in thin film used to take the slip system.

Fig 20 Thomason tetrahedral. Treat each {111} triangle as our local co-ordinate system.

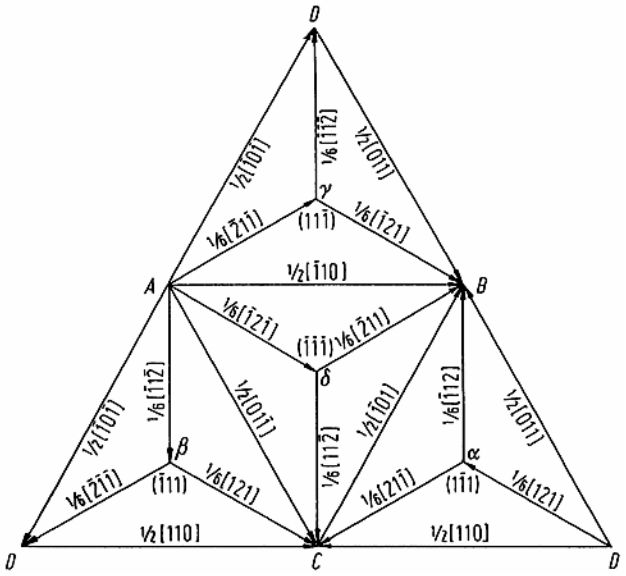

Fig.20 Thompson tetrahedron

Each sides of triangle are the burgers vector direction [18, 34, 35,40] . In the local x-y axis system, use Thomason tetrahedral to decide the two initial nodes of Frank Read source, as long as the connected dislocation line of two nodes can lie in our simulation thin film. Table 1 is the input dislocation source file based on all the condition and restrictions above. Because in the code it is dimensionless, the number of lattice constant is placing the role of length. So all the numbers which are not the slip system represent the number of lattice constant.

Take thickness equal to 1μm as example. The cutting method for this thin film is cutting 5μm cubic from 2μm to 3μm along [001] direction. So transfer the thickness 1μm to the number of lattice constant is equal to 2766. That means the "project length" on [001] cannot be greater than 2766.

Table 1 Dislocation source input information for 1μm thickness in "5μm" group

Defect kind	No. of plane	No. of nodes	Slip-plane miller	Burgers vector	Local slip plane-oringin	node local position
FR	1	2	[111]	[-0.5,0,0.5]	(3457.5,3457.5,6916.25)	(4000,-500)(-4000,-500)
FR	2	2	[-1-11]	[0.5,0,0.5]	(3457.5,10373.4,6916.25)	(4000,-500)(-4000,-500)
FR	3	2	[-111]	[0.5,0,0.5]	(10373.4,10373.4,6916.25)	(4000,-500)(-4000,-500)
FR	4	2	[1-11]	[-0.5,0,0.5]	(10373.4,3457.5,6916.25)	(4000,-500)(-4000,-500)

Then physically, our sources can make sense. Also in section 2.3.2 it is known those

dislocation configurations will not influence Hall-Petch size effect relationship [17].That is also good support about putting into dislocations from previous calculation result.

In order to have the same dislocation density for one simulation group with different grain size, for the $5\times5\times1\mu m^3$, 4 dislocation sources are input inside. Then 8 sources are input for $5\times5\times2\mu m^3$. The same principle can be used to the other size case.

For fix boundary condition, fig 21 is what dislocation looks like when it hits close boundary

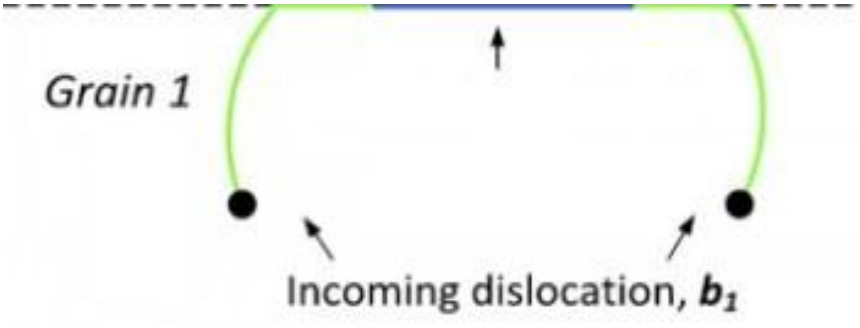

Fig. 21 Microstructure picture when dislocation motion is retricted by boundary

Directly, from equation (2), when the dislocation nodes move to the boundary, then set velocity to zero in the code. Based on the dislocation dynamics code, when the project node hits the boundary and there's no inertial force, let the previous time step node stop at the boundary. So the image of dislocation at that time will be like fig 22. And the close dislocation loop will form basically very tight in our thin film. Fig 23 is what it is.

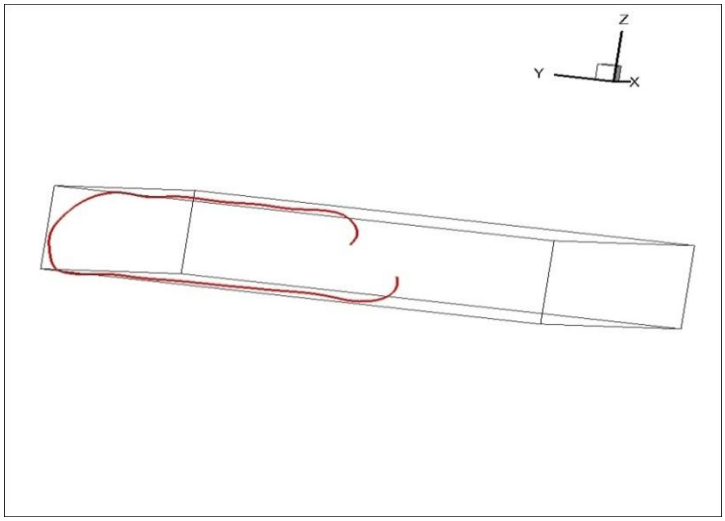

Fig.22 One edge dislocation move to fix-boundary microstructure picture

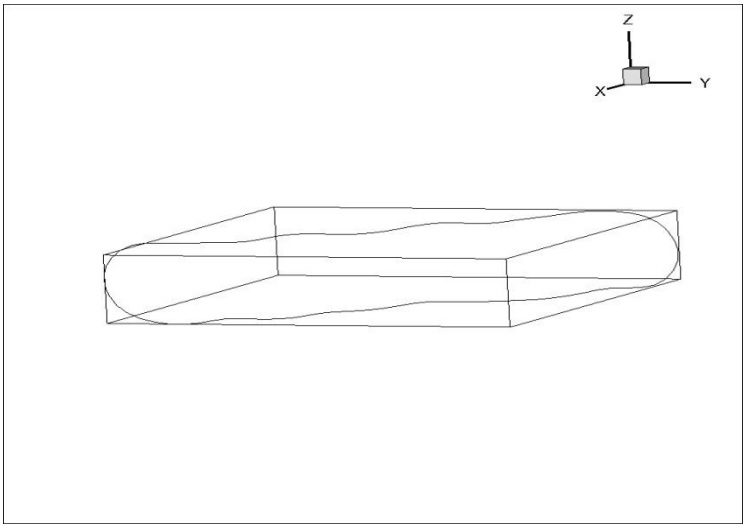

Fig.23 One entire dislocation loop held in the thin film.

CHAPTER 4

SOME INITIAL TESTS

4.1 Tension Test

Some basic mechanical simulations have been done to test the mechanical property of cubic Cu in micro scale. The parallel code used in the computation is called DeMecha. Single cubic crystal copper with dimensions of $2\times2\times2\mu m^3$ has been tested. The external load for this simulation is along [100] direction under a constant strain rate $10^{-2}s$. The original dislocation is distributed by Frank-Read source, with an initial dislocation density $\rho = 2.499\times10^{-2} cm/cm^3$. Other material constants used for the simulation for copper are: dislocation mobility=$1\times10^{-4} Pa/s$, shear modulus G=50GPa.

The strain in the simulation is S=strain rate $\times$ time step $\times$ N_time $\times$ times for loading. After 1600 iteration numbers loading, strain-stress curve is shown in fig 24.

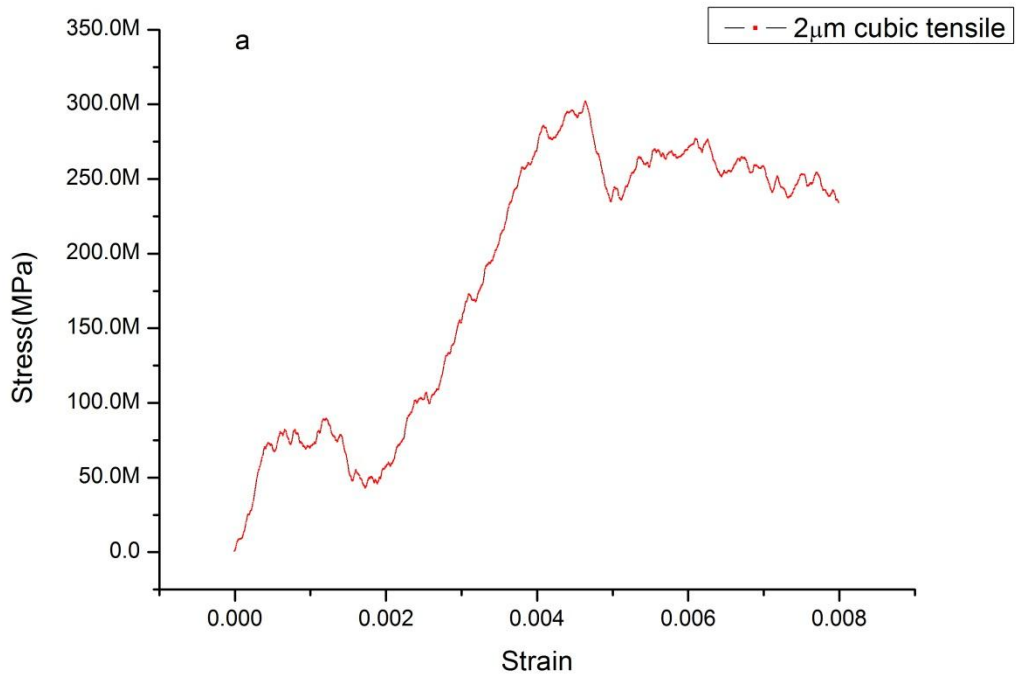

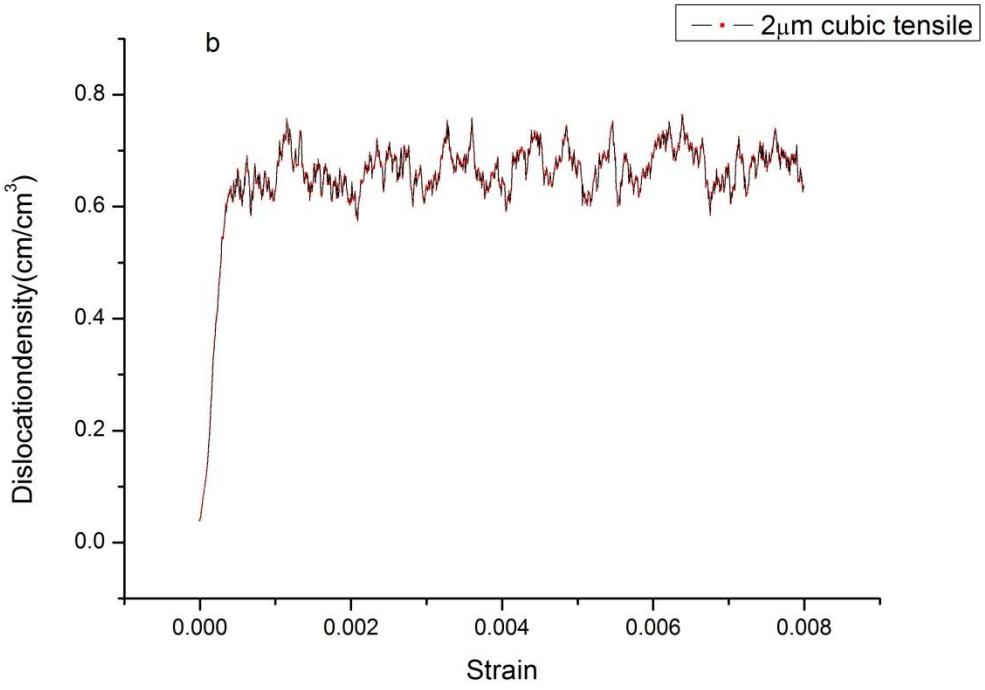

Fig. 24 The strain-stress curve for the simulation and dislocation density. (a) Strain-stress curve (b) dislocation density.

In the strain-stress curve, at the lower stress, the elastic deformation is dominant. However, at higher stress, the plastic deformation began to appear, where the strain went up to about 0.44%.

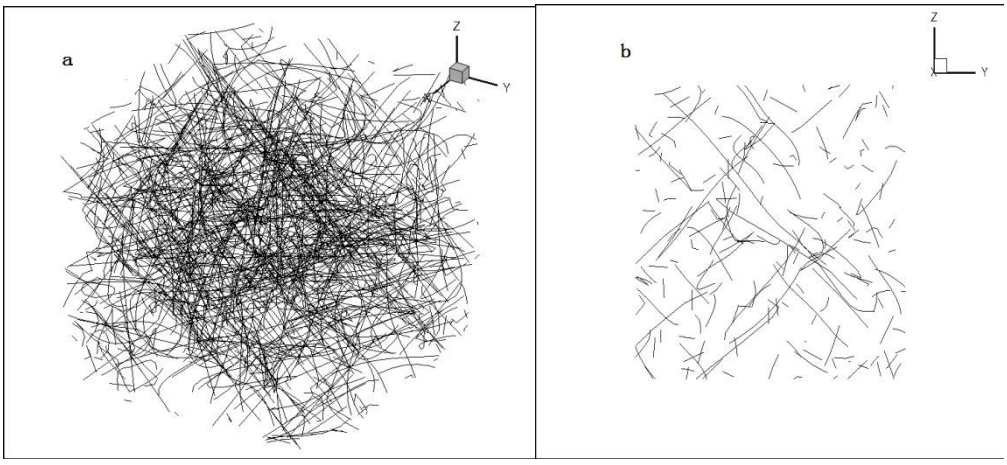

Fig. 25 The dislocation microstructure for 200 times loading. (a)the whole microstructure in 3D view.(b) one slice in Y-Z zone.

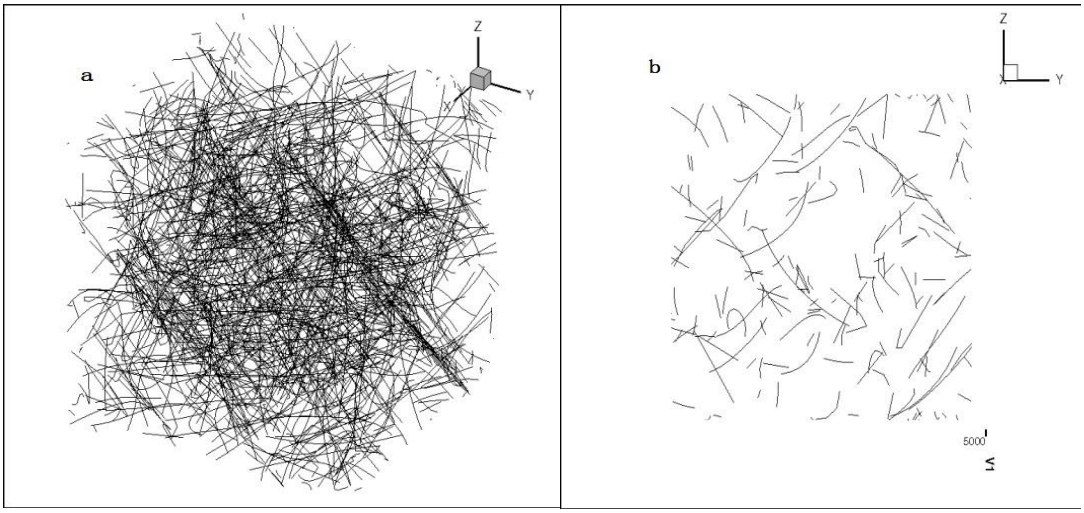

Fig. 26 The dislocation microstructure for 860 times loading. (a)the whole microstructure in 3D view. (b)one slice in Y-Z zone.

In the Fig 24, there are some zigzag areas in 200 times loading, 860 times loading, and 1560 times loading, which make the curve not as perfect as the theory curve. In order to understand the microstructure, the microstructure picture and one slice picture of these areas are plotted. In fig25, fig26, and fig27, the number of dislocation is decreasing. The reason of the phenomenon is dislocation annihilation. As the time goes on, dislocations begin to annihilate with each other. That reduces the number of dislocation [12, 26].

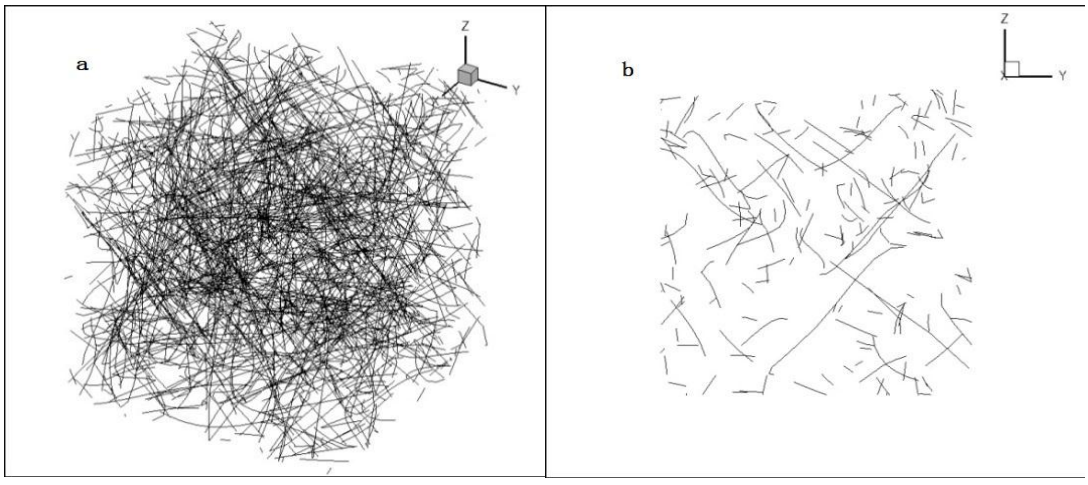

Fig. 27 The dislocation microstructure for 1560 times loading. (a)the whole microstructure in 3D view. (b)one slice in Y-Z zone

Therefore, for discrete dislocations, the parallel code DeMecha performs very well,

especially for the large-scale material computer simulation. The complex 3D model can be simplified and successfully simulated. In the simulation of the article, the $2\times2\times2\mu m^3$ single crystal copper performed plastic deformation at 0.44% loading. The result shows that the collective dislocation can explain the microstructure and strain-stress curve. Moreover, the dislocation annihilation might affect the stress hardening under some certain loading. It should be fixed better.

4.2 Cyclic Loading Test

Cyclic loading means the loading direction will periodically change as the time goes. Fig 28 shows how the loading direction becomes verse with time.

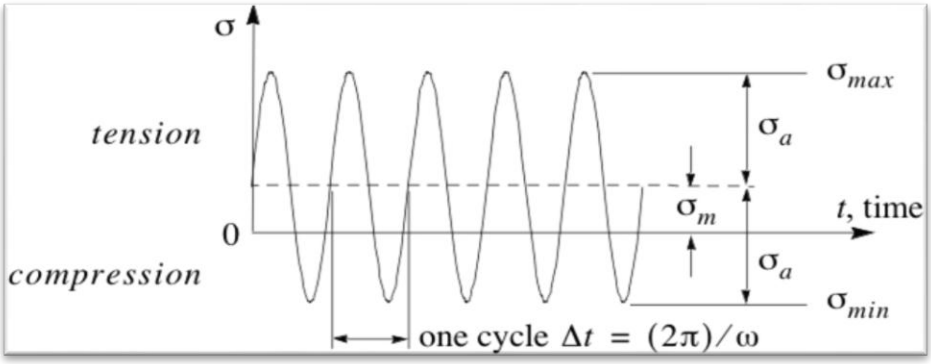

Fig.28 Stress vs. time mapping in cyclic loading

There's a significant physical phenomena caused by cyclic loading---fatigue. When material is suffering alternating stresses for a long period of time, fatigue will happen. Fatigue is a kind of localized structural damage which happens when material is subjected to cyclic loading. A very effective way to show time to failure for certain material is the S-N curve. That means stress verse cycles to failure, which when plotted stress amplitude, stress on the vertical axis and the logarithm of the number of cycles to failure on horizontal axis. The significance of the fatigue limit is as long as the material is loaded below this stress, it will not fail, no matter the number of times it is loaded. Material such as aluminum, copper and magnesium do not have a fatigue limit, so they will fail at any stress and number of cycles. The stress at which failure occurs for a given number of cycles is the fatigue strength--the number of cycles

required for a material to fail at a certain stress in fatigue life [25].

One more important feature in material deformation under cyclic loading is the Bauschinger effect. It means when metal is applied positive loading under deformation, after plastic deformation happens, reload it and get low hardening [37]. Fig 29 is a simple drawing of Bauschinger effect.

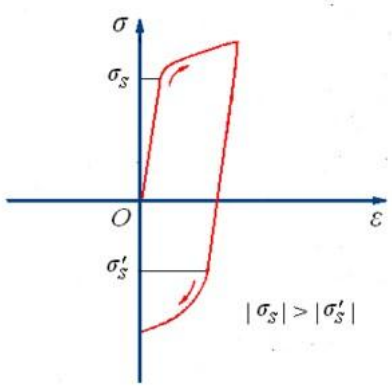

Fig. 29 Schematic illustration of the Bauschinger effect

About Bauschinger effect, there are two kinds of principal theory (Fig. 30), back stress theory and Orowan theory [54].Under the forward plastic deformation, moving dislocations will interact with different obstacles (like other dislocations, grain boundaries and precipitates). They prevent dislocations further propagation, which can generate a back stress around the contact point to stop further progress of similar signed dislocations. During the reverse deformation, this back stress repels the dislocations from the obstacles in the opposite direction, namely in the direction of reverse strain. Thus the back stress field will help to move the dislocation in the direction of reverse strain and the reverse yield stress drops by the level of the back stress (Fig. 30(a)). In an alloyed material, precipitated particles also act as interaction sites increasing the level of back stress(Fig.30(b)).

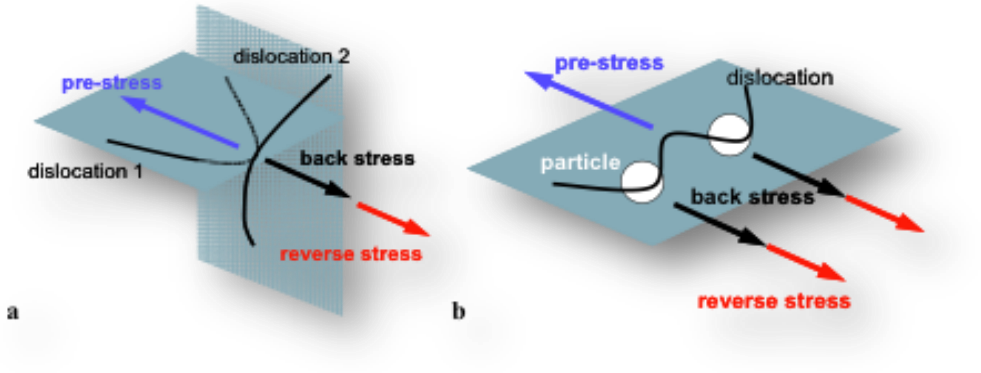

Fig. 30 Schematic representation of (a) Dislocation - Dislocation, (b) Dislocation - Particle interaction [54].

For this test, pick 2μm single crystal Cu in order to make the computing task small. And the strain rate is 102. Loading step is 1600, which means 400 steps positive loading, 800 steps negative loading and 400 steps positive reloading. Fig 31 is the strain-stress curve after deformation.

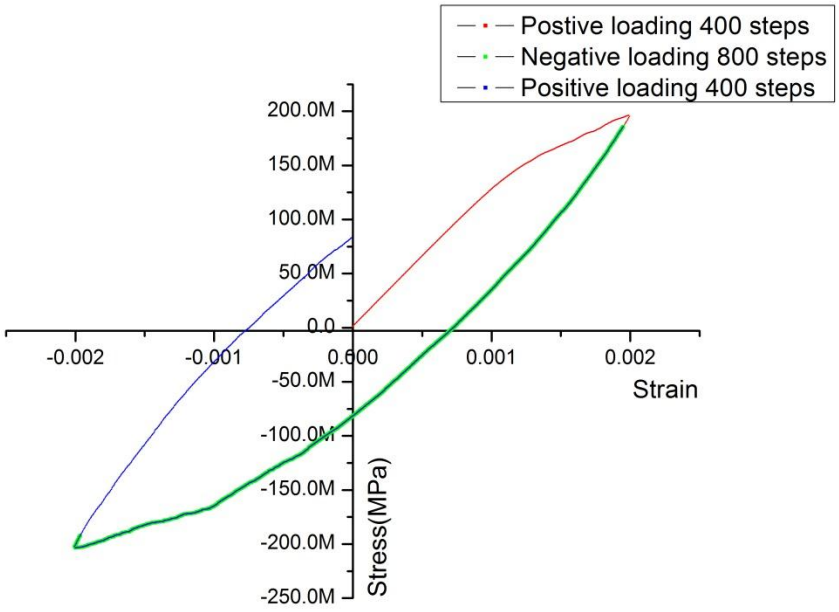

Fig. 31 Strain-stress curve for cyclic loading Cu after 1600 time steps.

The Bauschinger effect is very obvious when the time step goes to 800.Five particular areas on the strain-stress curve's dislocation microstructure are picked in order to have better understand, as shown in Fig 32.

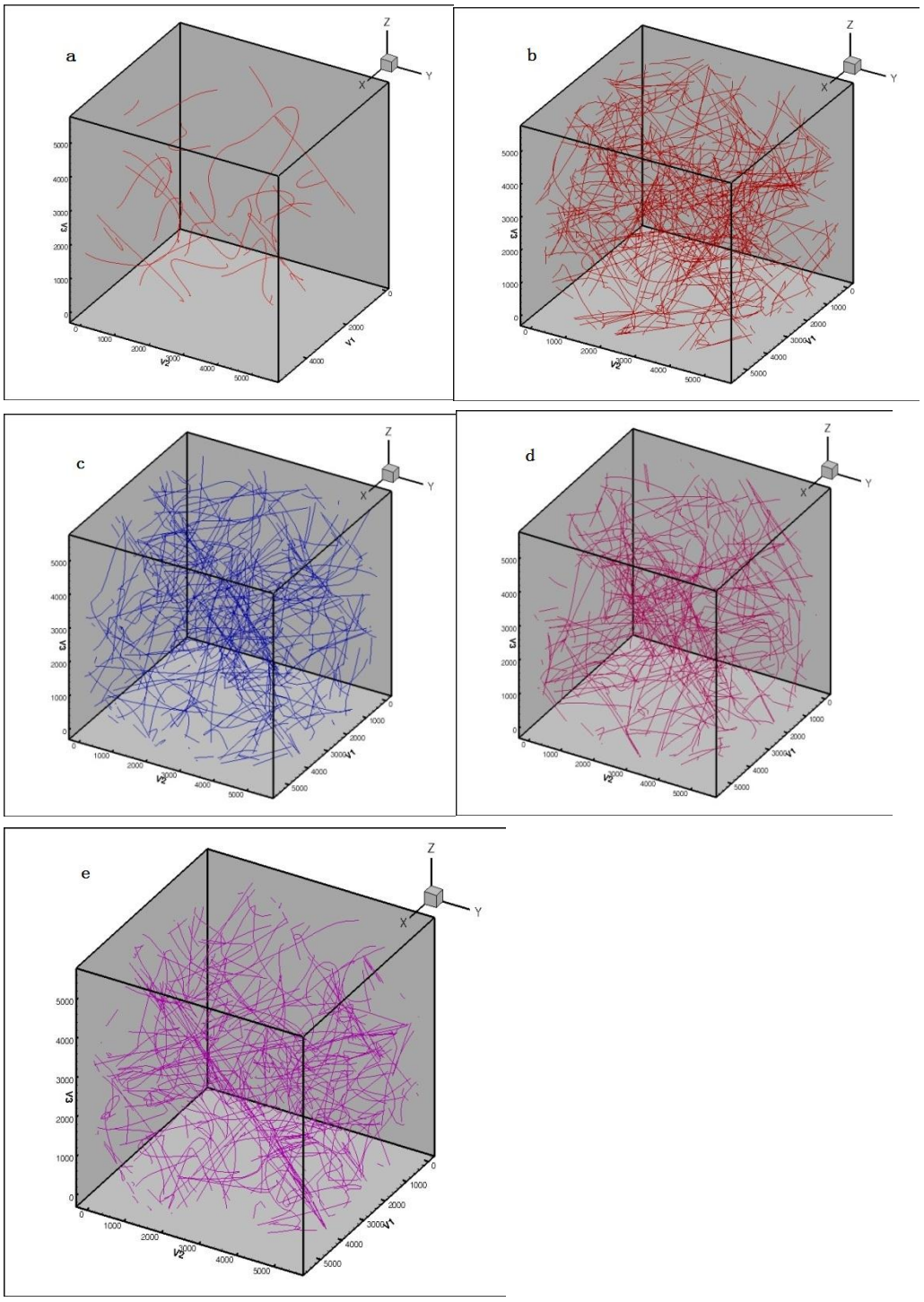

Fig. 32 Mircostructure picture for different loading time step. (a)20 (b)390 (c)750 (d)1190 (e)1950

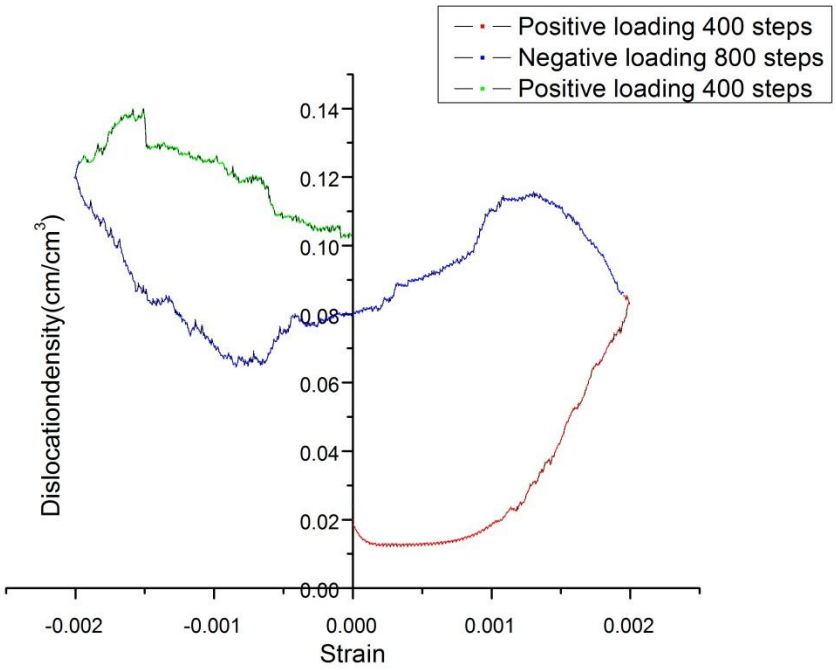

Fig. 33 Strain with dislocation density plot.

All the cases above were computed under the periodical boundary condition. The periodical boundary condition is a good model to use small simulation size to reflect the mechanical and microstructure property for large size material application. When a dislocation move out of the simulation shape, the part out of simulation shape will be erased and mapped back to the other co-respond position inside the shape.
Based on all those evidence, it is concluded that under the setting condition, the single crystal Cu will appear elastic deformation if the strain goes up to about 0.44%. And they are so many “wave” in strain-stress curve, looked a little unstable on the data; the reason may be the dislocation annihilation which probably make the strain-stress curve not as “perfect” as fluent curve.

CHAPTER 5

SIMULATION RESULT

The simulated loading direction is [100]. Strain rate equals to 1000 per second. Total iteration loop numbers are 3000. Delta time is $2\times10^{-11}s$. Other information of simulation condition can be found in section 3.4 and Table 1. Initially, fig 34 below is the position of dislocation sources (for $5\times5\times1\mu m^3$ case).

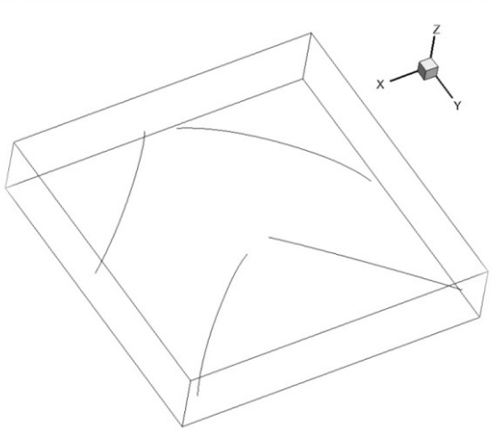

Fig. 34 Initial dislocation sources position for $5\times5\times1\mu m^3$ case

The reason of putting dislocation sources as this manner is, we hope the dislocation line is longer enough. Therefore, it is much easier for them to interact with grain boundary and other dislocations. That's why screw dislocation is chosen for the simulation instead of edge dislocation under previous loading direction, the geometry position of source is parallel to the top and bottom surface along [001] direction.
In order to make sure all the cases tested have the same initial dislocation source density, the same dislocation length for the group of case is kept for different simulation thickness, but increases the number of sources, which is proportional to the thin film thickness, as shown in Fig 35.

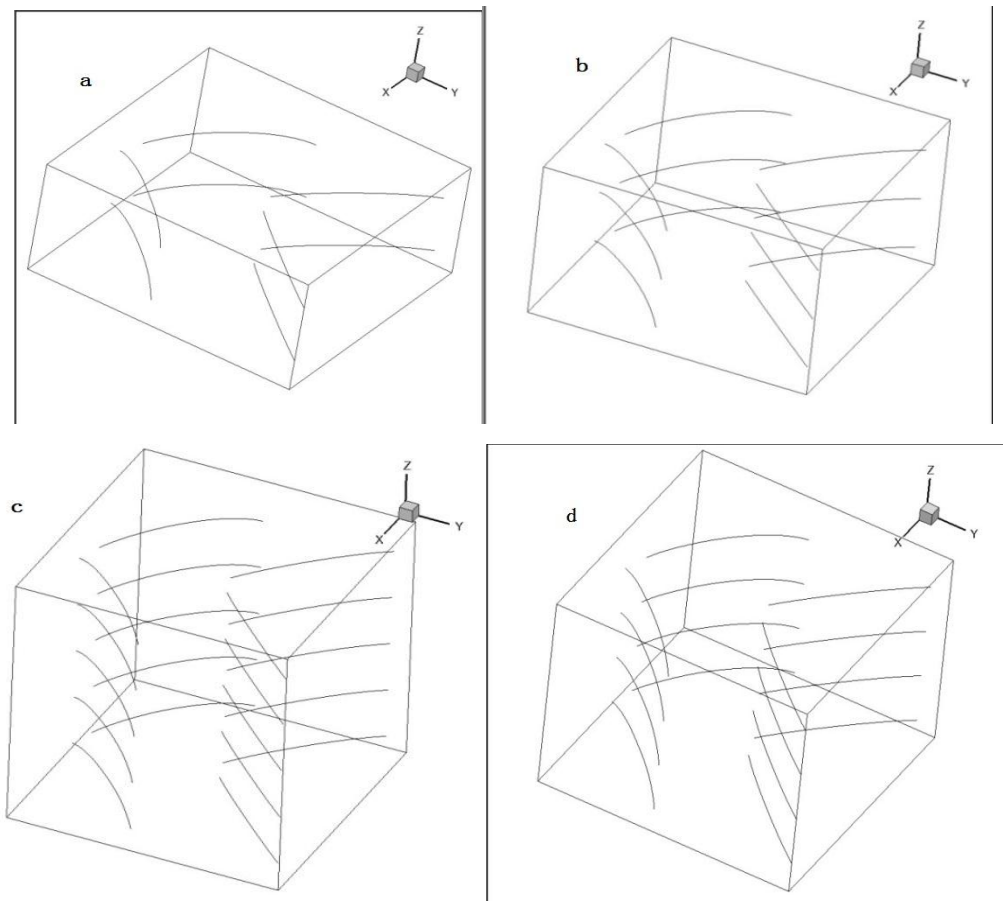

Fig. 35 Dislocation source positions for different 5μm case thin film—(a)2μm thickness (b) 3μm thickness (c) 4μm thickness (d) 5μm thickness

After the calculations, the group strain-stress curve is plotted together, as shown in Fig 36 below.

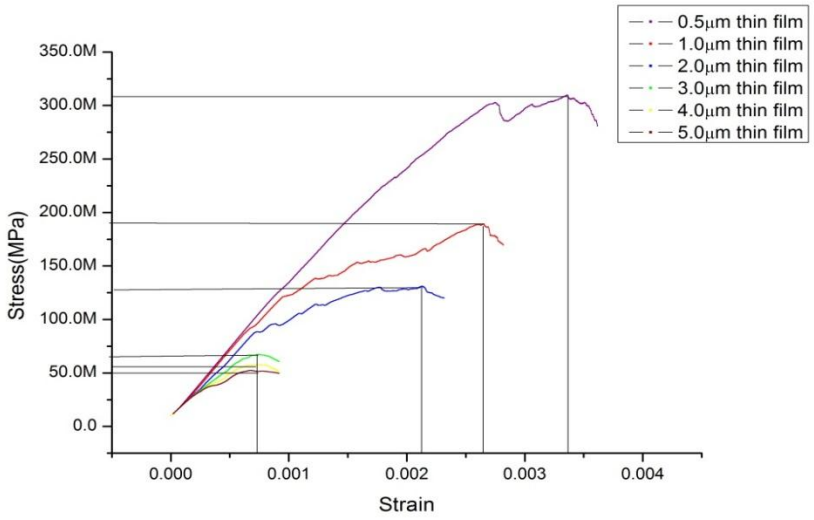

Fig.36 strain-stress comparison for $5\times5\times x\mu m^3$

In order to have good comparisons, another simulation is introduced which the thickness is smaller than 1μm ---0.5μm. It is shown that for smaller thickness, they have large max plastic stress. Also when the thickness is larger, the plastic strain is very close. The critical strains from 0.5μm case to 5μm case are 0.0033, 0.0026, 0.0021, and 0.0007, respectively. 3μm, 4μm and 5μm thin film have the same critical strain-0.0007.

Fig 37 is dislocation microstructure for strain equal to 0.0033 of $5\times5\times0.5\mu m^3$. Basically, for each thin film, the max plastic stress always co-responds to relative microstructure---lots of dislocation pile-up at the boundary, and form very dense dislocation close loop held tightly by boundary.

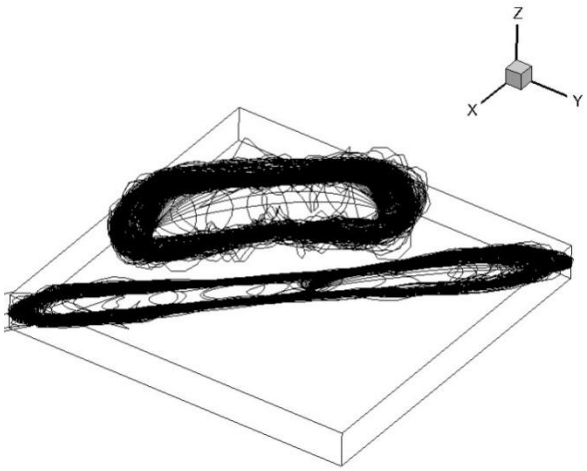

Fig. 37 Dislocation microstructure for 0.5μm thickness on max plastic stress

For strain equals to 0.0026, 1μm case achieves the max plastic stress, but the stress of 2μm case begins to decrease due to more dislocation activation and motion. When strain equals to 0.0021, 1μm case plot has not reached the max plastic value, but 2μm case has reached. The comparison of the two case microstructure (when the iteration loop time reaches 1050) is shown in fig 38.

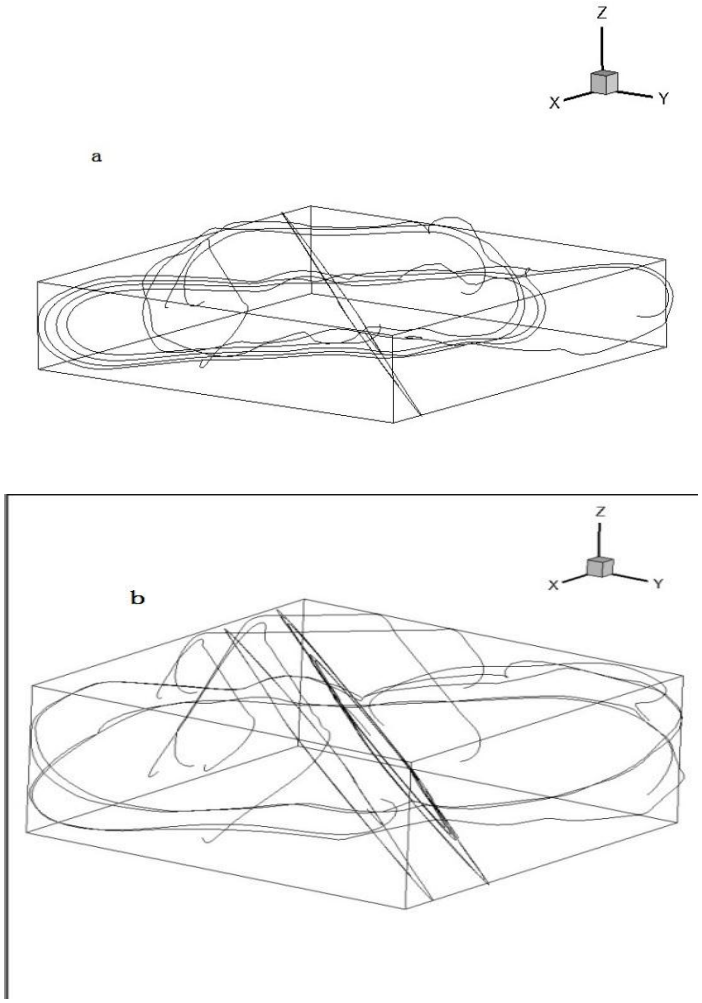

Fig. 38 Dislocation microstructure comparison when strain=0.0021. (a)1μm case (b) 2μm case

Initially, there are 4 sources in 1μm film and 8 sources in 2μm film. In fig 38, there are 8 dislocations in 1μm film case and 16 dislocations in 2μm film case which means more dislocations are activated in thicker film. Also, the dislocation microstructure in 1μm case is more stable than 2μm case. It can be concluded that maximum plastic region is formed due to large dislocation motion.

For almost the same strain, 3, 4, 5μm cases also have close plastic stress. Fig 39 is the comparison for those 3 cases.

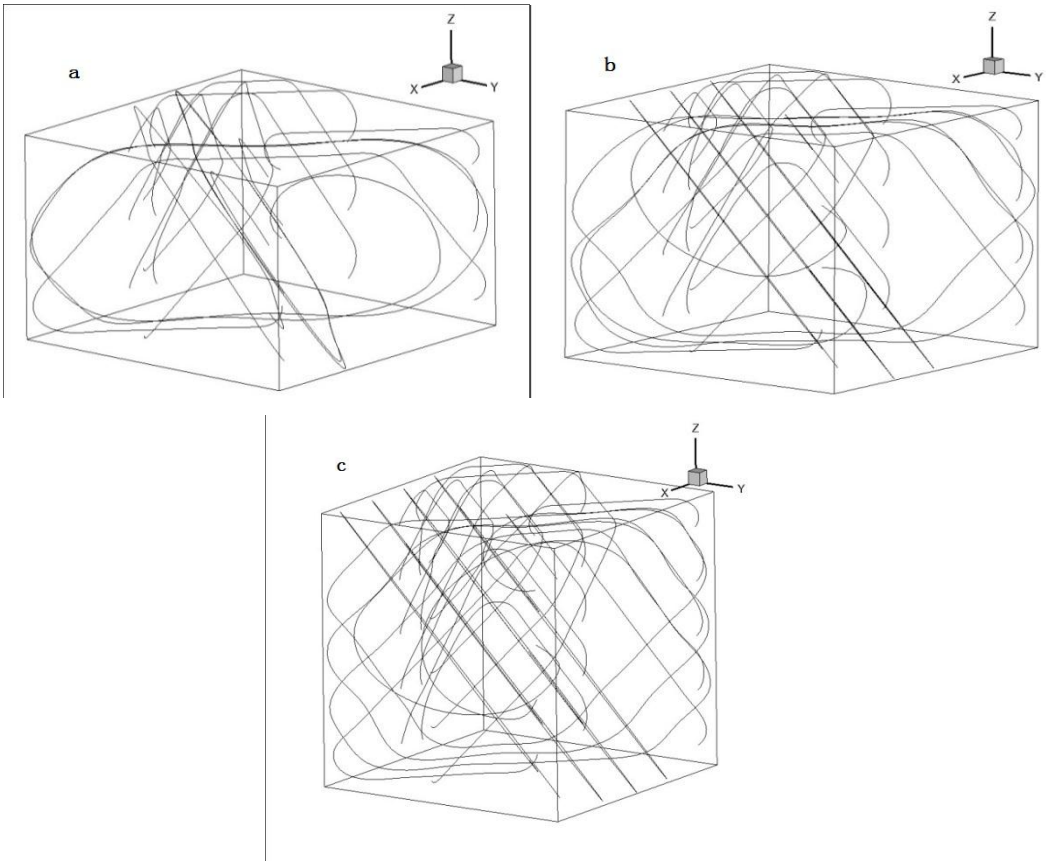

Fig. 39 dislocation microstructure comparison when strain=0.0007 for (a)3μm case (b)4μm case (c)5μm case

Initially, there are 12 sources in 3μm case, 16 sources in 4μm case, and 20 sources in 5μm case. However, when they reached their maximum plastic stress value, the numbers of dislocations in thin films are 13, 17, and 21, respectively. So it can be concluded that for thicker film, plastic area does not have a strong dependence to dislocation nucleation. In other words, dislocation pile-up and nucleation are the dominant factors for thinner film plastic deformation. Also for thicker film, plastic strain is smaller than thinner film. The thicker the films are, the closer plastic strain is. To make sure the principle can apply other case, a group of thin films has been tested. They follow the same test condition and the dislocation source input method. Fig 40 is the position of how we place dislocation sources in 10μm cases.

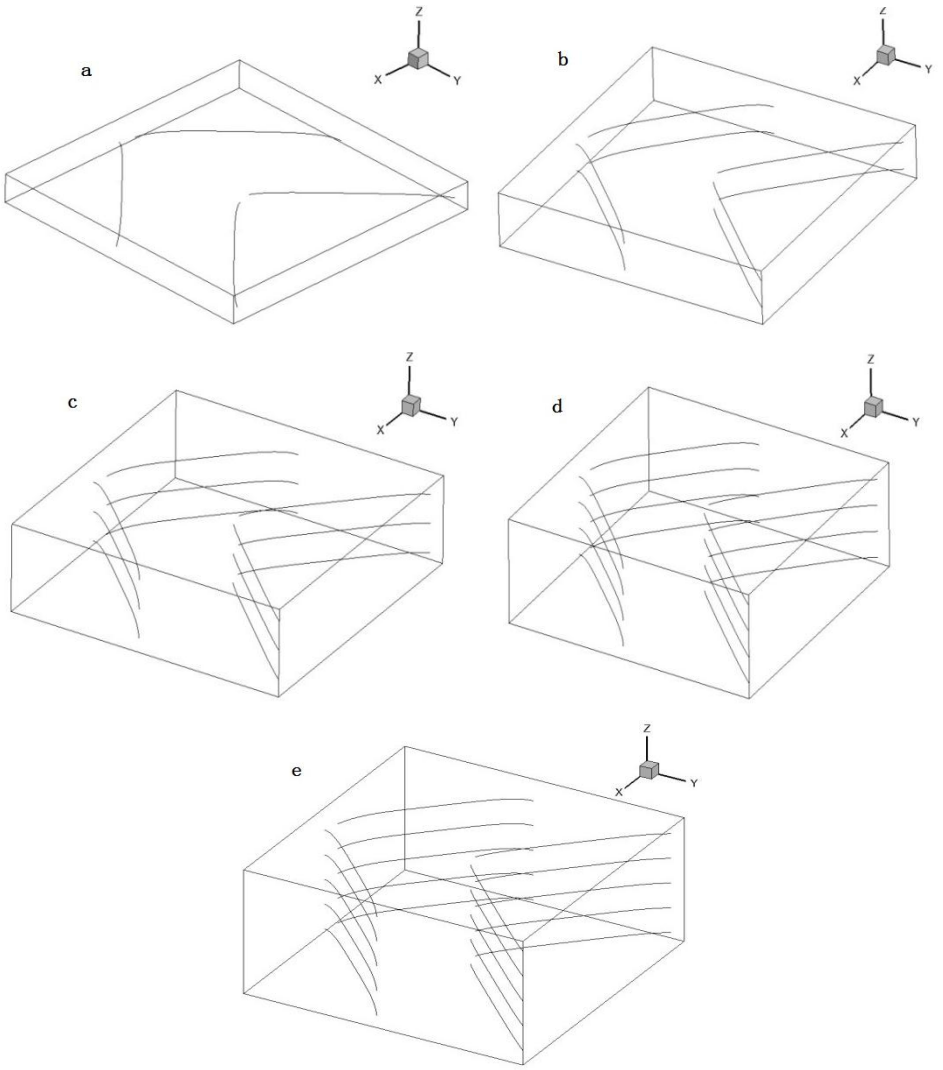

Fig. 40 Initial dislocation sources position of $10\ 10\mu\times\times x\ \ m^{3}$ for (a)1μm (b)2μm (c)3μm (d)4μm (e)5μm

The dislocation density for this group is $1\times10^{7}\,cm/cm^{3}$ which is the half of the dislocation density in 5μm case.

Other simulation conditions are the same with previous simulation. Fig 41 is the combined strain-stress curve for the entire 10μm cases test. The critical strains from 1μm case to 5μm case are 0.003, 0.0023, 0.00075 and 0.0007, respectively.2μm and 3μm cases have the same critical strain-0.0023.

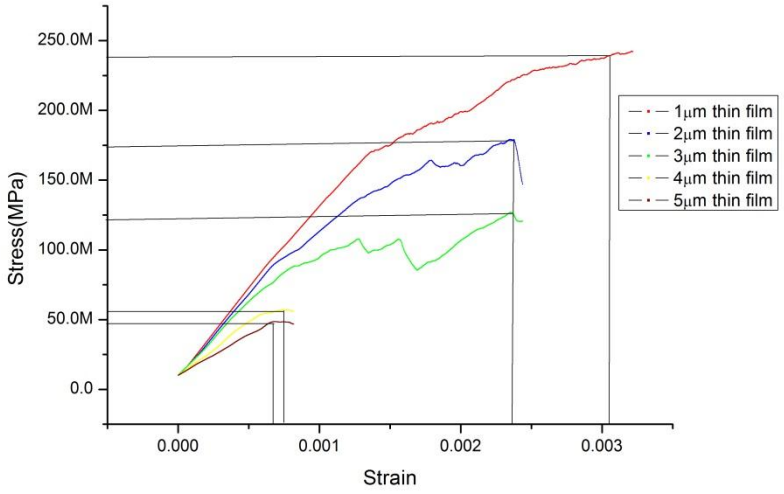

Fig. 41 strain-stress comparison for

Similarly from 5μm group, there's noticeable size effect in 10μm group. In this group, both 2μm and 3μm cases have the same plastic strain. So do the 4μm and 5μm.

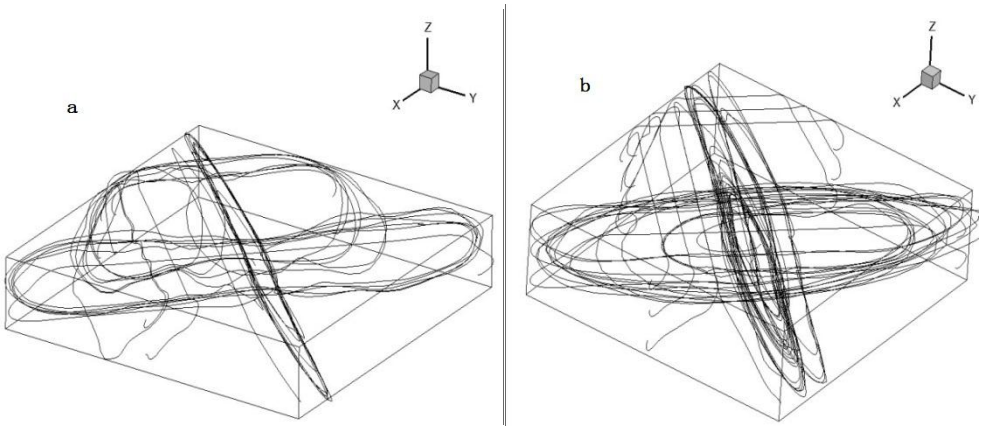

Fig. 42 Dislocation microstructure comparison when strain=0.0023 for (a)2μm case (b)3μm case

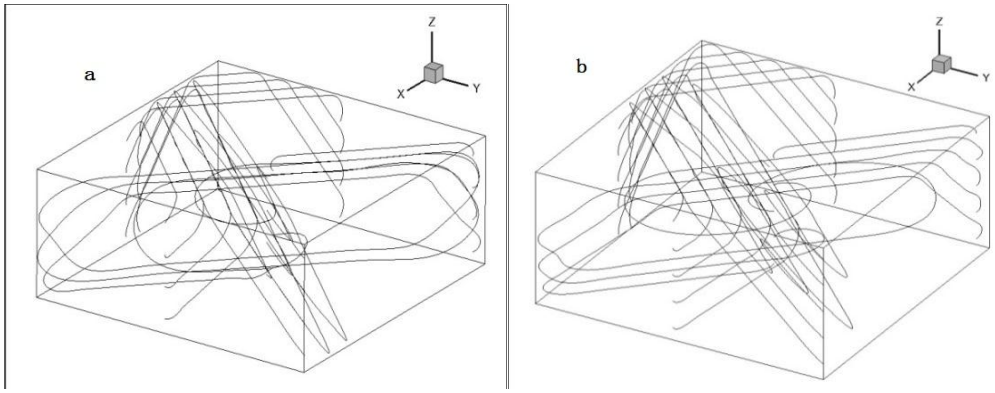

Fig. 43 Dislocation microstructure comparison when strain=0.0007 for (a)4μm case (b)5μm case

For fig 42, in the beginning, there are 8 sources in 2μm film and 12 sources in 3μm film. When deformation continues, there are 19 dislocations in 2μm film and 30 dislocations in 3μmfilm. This is very similar with what we found in 5μm cases group. Usually, plastic deformation has close relationship with large number of dislocation motion. Under the same plastic strain, thicker film has lower plastic stress.
Also for fig 43, there's no large number increase of dislocation. We still cannot observe very obvious dislocation pile-up and moving action.

Table 2 Simulation data of comparison

5μm group(μm)thickness	Max plastic stress(MPa)	10μm group(μm)thickness	Max plastic stress(MPa)
1	189	1	250
2	131	2	179
3	67.2	3	120
4	57.5	4	57.7
5	50	5	45.8

Based on simulation data (Table 4.1) and experimental data from Xiang's paper (Fig 3.), Fig 44 is the comparison plot for thickness vs. max-plastic stress/yield stress. From fig 44 we can find that all the cases show strong size effect. And Fig 3 shows that in experiment, smaller thickness films also have smaller grain size.

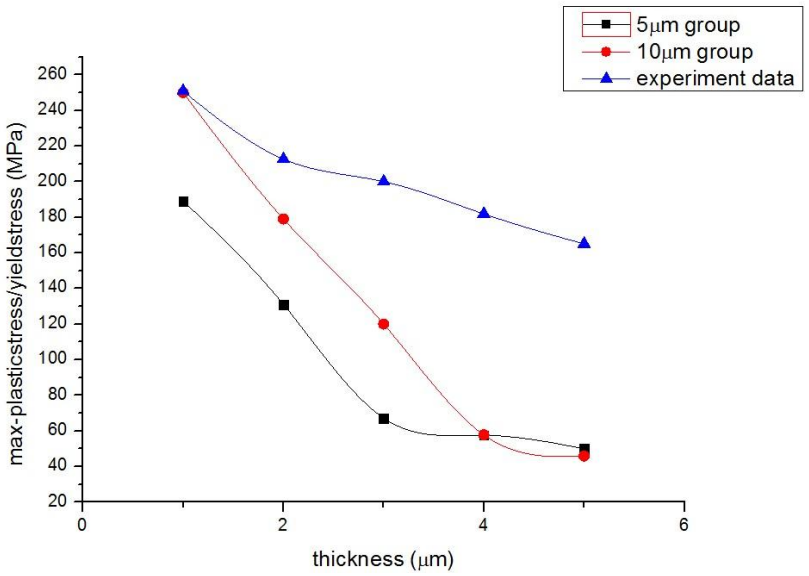

Fig. 44 Comparison plot between simulation data and experimental data

Fig 44 shows strong size effect and also that in smaller size thin films, the difference between yield strength and our maximum plastic stress is close (as material yield strength is always a little smaller than maximum plastic stress). When the size is large enough, the difference could be very large. For thinner films, dislocations are easier to pile-up at the boundary. However, for thicker films, different dislocation density will result in huge number of dislocation pile-ups. Thus, we can conclude that for thicker film, contribution of dislocation motion to plasticity will be less than for thinner film.

CHAPTER 6

CONCLUSIONS

The dislocation dynamics simulation method has already become a powerful tool in material plastic deformation modeling. It can be used to solve almost all regular simulation material shapes and is still being developed to fit boundaries and precipitate problems in the simulation setup. In this thesis, focus on thin film technology and its associated mechanical properties. The size effect has already been observed in experiments and ultimately leads to a need for a better simulation which correlated increasing decreasing thickness. Understanding of the contribution of dislocation theory on size effect, 2D cases have been investigated extensively, experimentally through simulations; have been shown to be effective modeling the size effect. In this thesis, 3D simulations have been proposed to test copper thin film and have shown similarly good results. In order to fit realistic applications, we set the grain boundaries as impenetrable, which means dislocation motion is restricted at the boundaries. Two simulation groups have been examined (1)5 $\mu m^3$and (2)10 μm cases. Screw dislocations are input as the initial source. From the simulations of these two cases of thin film dislocation dynamics, the size effect has a strong relationship with dislocation motion, especially for thinner films. For thicker films, plastic area does not have a strong dependence on dislocation nucleation. In other words, dislocation pile-up and nucleation are the dominant factors for thinner film plastic deformation. Also for thicker films, plastic strain is smaller than thinner films.

CHAPTER 7

FUTURE WORK

Based on comparisons between experimental and simulation data, there are some interesting areas which need be further studied. The simulations presented here cover only the single grain case. Grain boundary interactions with dislocations is a main aspect of the current research which needs to be considered in this image force and close boundary model. Multi-grain case simulation requires large dislocation-grain boundary interactions in addition to dislocation-dislocation interactions. Also, precipitates a model accounting for the variation in precipitate size would be more realistic. From dislocation theory, we know that, for small precipitates, size dislocations can cut through precipitates and continue its motion. For large size precipitates, dislocation motion will be restricted at the precipitate; forming close dislocation loops at the precipitate, and other parts of dislocation line will re-combine together and continue its motion. Another interesting model which we have to consider is large precipitates with dislocations inside them or dislocation simulations for metal alloys. If the precipitate material and bulk material have different crystal systems and different slip systems, two kinds of slip rules are required. Also, for fcc, bcc, and hcp slip systems, how to treat dislocation motion in different slip systems when it hits the boundary and how to calculate the force when dislocation in different slip system (different atoms) move close to each other are two main challenges need to be solved.

REFERENCES

[1] V.S. Deshpande, A. Needleman, E. Van der Giessen, 2005, Plasticity size effects in tension and compression of single crystals, Journal of the Mechanics and Physics of Solids. 53 (2005) 2661–2691

[2] Caizhi Zhou, Richard LeSar, 2011, Dislocation dynamics simulations of plasticity in polycrystalline thin films, International Journal of Plasticity. 30–31 (2012) 185–201

[3] L. Nicola, Y. Xiang, J.J. Vlassak, E. Van der Giessen, A. Needleman, 2006, Plastic deformation of freestanding thin films: Experiments and modeling, Journal of the Mechanics and Physics of Solids. 54 (2006) 2089–2110

[4] Nasr M. Ghoniem and L. Z. Sun, 1999, Fast-sum method for the elastic field of three-dimensional dislocation ensembles, Phys. Rev. B, 60(1):128, 1999.

[5] Zhiqiang Wang, Nasr Ghoniem, SriramSwaminarayan, Richard LeSar, 2006, A parallel algorithm for 3D dislocation dynamics, Journal of Computational Physics 219 (2006) 608–621

[6] N.M.Ghoniem, S.H.Tong, and L.Z.Sun, Parametric dislocation dynamics: A thermodynamics-based approach to investigations of mesoscopic plastic deformation,Phys. Rev. B, 61:913, 2000.

[7] Jianming Huang and Nasr M Ghoniem, 2002, Accuracy and convergence of parametric dislocation dynamics, ModellingSimul.Mater. Sci. Eng. 10 (2002) 1–19

[8] Zhiqiang Wang, Rodney J.McCabe, Nasr M. Ghoniem, Richard LeSar, AmitMisra, Terence E. Mitchell, 2003, Dislocation motion in thin Cu foils: a comparison between computer simulations and experiment, ActaMaterialia 52 (2004) 1535–1542

[9] L. Nicola, E. Van der Giessen, A. Needleman, 2001, 2D dislocation dynamics in thin metal layers, Materials Science and Engineering A309–310 (2001) 274–277

[10] M. Sauzay, L.P. Kubin, 2011, Scaling laws for dislocation microstructures in monotonic and cyclic deformation of fcc metals, Progress in Materials Science 56 (2011) 725–784

[11] Zhiqiang Wang, 2004, Large Scale Dislocation Dynamics Simulation of Bulk Deformation, Ph.D. thesis, University of California, Los Angeles

[12] B. Devincre, L.P. Kubin, Simulations of forest interactions and strain hardening in fcc crystals, ModellingSimul. Mater. Sci. Eng. 2 (1994) 559

[13] K.W. Schwarz, Simulation of dislocations on the mesoscopic scale. i. Methods and examples, J. Appl. Phys. 85 (1) (1999) 108–119.

[14] R. M. Niu, G. Liu, C. Wang, G. Zhang, X. D. Ding, J. Sun, 2004, Thickness dependent critical strain in Cu films adherent to polymer substrate.Appl. Phys. Lett. **90**, 161907 (2007)

[15] Y. Xiang, J.J. Vlassak, 2006, Bauschinger and size effects in thin-film plasticity, ActaMaterialia 54 (2006) 5449–5460

[16] N. A. Flect, G. M. Muller, M. F. Ashby and J. W. Hutchinson, 1993, Strain gradient plasticity: theory and experiment

[17] S. B. Biner and J. R. Morris, 2003, The effects of grain size and dislocation source density on the strengthening behavior of polycrystals: a two-dimensional discrete dislocation simulation, Philisophical Magazine, vol. 83, Issue 31, p.3677-3690

[18] J. P. Hirth, Theory of dislocation,1982, (New York: McGraw-Hill)

[19] N.M. Ghoniem and R. Amodeo. Computer simulation of dislocation pattern formation. Solid State Phenomena, 3 & 4:377, 1988.

[20]Hussein M. Zbib, Moono Rhee, and John P. Hirth. On plastic deformation and the dynamics of 3d dislocations. Int. J. Mech. Sci., 40(2-3):113{127, 1998.

[21] Benoit Devincre and Ladislas P. Kubin. The modelling of dislocation dynamics: Elastic behavior versus core properties. Philosophical Transactions: Mathematical, Physical and Engineering Sciences, 355(1731):2003, 1997.

[22] M. Rhee, H.M. Zbib, J.P. Hirth, H. Huang, and T. Rubia. Models for long-/short-range interactions and cross slip in 3d dislocation simulation of bcc single crystals. ModellingSimul.Mater.Sci. Eng., 6:467{492, 1998.

[23]M.C. Fivel, T.J. Gosling, and G.R. Canova. Implementing image stresses in a 3d dislocation simulation. ModellingSimul.Mater. Sci. Eng., 4:581{596, 1996.

[24] M. Fivel, M. Verdier, and G. Canova. 3d simulation of a nanoindentation test at a mesoscopic scale. Materials Science and Engineering, A234-236:923, 1997.

[25] C. Depres, C.F. Robertson, and M.C. Fivel. Low-strain fatigue in 316l steel surface grains: a three dimensional discrete dislocation dynamics modelling of the early cycles. part-1: Dislocation microstructures and mechanical behaviour. Phil. Mag., 84(22):2257, 2004.

[26] T.A. Khraishi and H.M. Zbib. Free surface effects in 3d dislocation dynamics: formulation and modeling. J. Eng. mat. Tech. (JEMT), 124(3):342,2002.

[27] H. Yasin, H.M. Zbib, and M.A. Khaleel. Size and boundary effects in discrete dislocation dynamics: coupling with continuum finite element. Mateiral Science and Engineering, A309-A310:294, 2001

[28] Hussein M. Zbib and T.D. Rubia. A multiscale model of plasticity: Patterning and localization. Society of Materials Science of Japan, A:341, 2001.

[29] K.W. Schwarz. Simulation of dislocation on the mesoscopic scale. ii. application to strained-layer relaxation. Journal of Applied Physics, 85(1):120, 1999.

[30] K.W. Schwarz and D. Chidambarrao.Dislocation dynamics near film edge and corners in silicon. Journal of Applied Physics, 85(10):7198, 1999.

[31] Wei Cai and et al. Massively parallel dislocation dynamics simulations. In IUTAM Symposium on Mesoscopic Dynamics of Fracture Process and Material Strength, Osaka, Japan, July 7-11 2003. Kluwer Academic Publisher.

[32] Georey H. Campbell, Stephen M. Foiles, Hanchen Huang, Darcy A. Hughes, Wayne E. King, David H. Lassila, Daniel J. Nikkel, John Y. Shu, and Valery P. Smyshlyaev. Multi-scale modeling of polycrystal plasticity: a workshop report. Materials Science and Engineering, A251:1{22, 1998.

[33] T. Diaz de la Rubia and V.V. Bulatov. Materials research by means of multiscale computer simulation. MRS Bulletin, 26(3):169{175, 2001.

[34] Erik Nes. Modelling of work hardening and stress saturation in fcc metals. Progress in Materials Science, 41:129{193, 1998.

[35] F.R.N. Nabarro. Work hardening of face-centered cubic single crystals. Strength of Metals and Alloys, 3:1667, 1985.

[36] R. Martinez and N. M. Ghoniem. The influence of crystal surfaces on dislocation interactions in mesoscopic plasticity: A combined dislocation dynamics-finite element approach. J. Comp. Meth. Engr. Science, CMES, 3(2):229, 2002.

[37] E.A. Repetto and M. Ortiz. A micromechanical model of cyclic deformation and fatigue-crack nucleation in fcc single crystals. Acta.Mater., 45(6):2577, 1997.

[38] E.H. Yoe. A dislocation at a free surface. Philosophical Magazine, 6:1147, 1961.

[39] P.P. Groves and D.J. Bacon.The dislocation loop near a free surface. Philosophical Magazine, 22:83, 1970.

[40] D. Hull and D.J. Bacon. Introduction to Dislocations.Pergamon Press, 3 edition, 1984.

[41] A. El-Azab and N.M. Ghoniem. Green's function for the elastic

[42] N.M. Ghoniem and J.M. Huang. Computer simulations of mesoscopic plastic deformation with differential geometric forms for the elastic field of parametric dislocations. Review of recent progress. J. de Physique, 11(5):53, 2001.

[43] G. Holzapfel. Nonlinear Solid Mechanics.Chichester, West Sussex:Wiley, 2000.

[44] Marc Snir, Steve Otto, Steven Huss-Lederman, David Walker, and Jack Dongarra.MPI|The Complete Reference, volume 1. The MIT Press, 2nd edition, 1998.

[45] William Gropp, Ewing Lusk, and Anthony Skjellum. Using MPI: Portable Parallel Programming with the Message-Passing Interface. The MIT Press, 1994.

[46] Jaswinder Pal Singh, Chris Holt, Takashi Totsuka, Anoop Gupta, and John Hennessy. Load balancing and data locality in adaptive hierarchical n-body methods: Barnes-hut, fast multipole, and radiosity. Journal of Parallel and Distributed Computing, 27:118, 1995.

[47] H.Y. Wang and R. Lesar.O(n) algorithm for dislocation dynamics. Philosophical Magazine A, 71(1):149, 1995.

[48] Jui-Lin Lu and Daniel I. Okunbor. Parallel implementation of 3d fma using mpi. Proceedings of Second MPI Developer's Conference, page 119, 1996.

[49]L. Greengard and V. Rokhlin.A fast algorithm for particle simulations. Journal of Computational Physics, 73:325{348, 1987.

[50] Carl E. Pearson. Numerical Methods in Engineering And Science. Van

Nostrand Reinhold Company, New York, 1986.

[51] B.W. Lagow, I. M. Robertson, M. Jouiad, D. H. Lassila, T. C. Lee, and H. K. Birnbaum.Observation of dislocation dynamics in the electron microscope. Mat. Sci. Engin. A, 309:445, 2001.

[52] M.C. Fivel, C.F. Robertson, G.R. Canova, and L.Boulanger.Threedimensional modelling of indent-induced plastic zone at a mesoscale. Acta.Mater., 46(17):6183, 1998.

[53] U.F. Kocks H. Mecking and Ch. Hartig. Taylor factors in materials with many deformation modes. ScriptaMaterialia, 35:465, 1996.

[54] L.M. Brown, Orowan's explanation of the Bauschinger effect, ScriptaMetallurgica, Vol. 11, 1977, p. 127 – 131.